

DA-LSTM: A Dynamic Drift-Adaptive Learning Framework for Interval Load Forecasting with LSTM Networks

Firas Bayram^a, Phil Aupke^a, Bestoun S. Ahmed^{a,e}, Andreas Kassler^{a,d}, Andreas Theocharis^b and Jonas Forsman^c

^aDepartment of Mathematics and Computer Science, Karlstad University, Karlstad, 65188, Sweden

^bDepartment of Engineering and Physics, Karlstad University, Karlstad University, Karlstad, 65188, Sweden

^cAdvanced Analytics Solution, CGI, Karlstad, 65224, Sweden

^dFaculty of Computer Science, Deggendorf Institute of Technology, Deggendorf, 94469, Germany

^eDepartment of Computer Science, Faculty of Electrical Engineering, Czech Technical University in Prague, Prague, 16627, Czech Republic

ARTICLE INFO

Keywords:

Interval load forecasting

Concept drift

Adaptive LSTM

Change-point detection

Dynamic drift adaptation

ABSTRACT

Load forecasting is a crucial topic in energy management systems (EMS) due to its vital role in optimizing energy scheduling and enabling more flexible and intelligent power grid systems. As a result, these systems allow power utility companies to respond promptly to demands in the electricity market. Deep learning (DL) models have been commonly employed in load forecasting problems supported by adaptation mechanisms to cope with the changing pattern of consumption by customers, known as concept drift. A drift magnitude threshold should be defined to design change detection methods to identify drifts. While the drift magnitude in load forecasting problems can vary significantly over time, existing literature often assumes a fixed drift magnitude threshold, which should be dynamically adjusted rather than fixed during system evolution. To address this gap, in this paper, we propose a dynamic drift-adaptive Long Short-Term Memory (DA-LSTM) framework that can improve the performance of load forecasting models without requiring a drift threshold setting. We integrate several strategies into the framework based on active and passive adaptation approaches. To evaluate DA-LSTM in real-life settings, we thoroughly analyze the proposed framework and deploy it in a real-world problem through a cloud-based environment. Efficiency is evaluated in terms of the prediction performance of each approach and computational cost. The experiments show performance improvements on multiple evaluation metrics achieved by our framework compared to baseline methods from the literature. Finally, we present a trade-off analysis between prediction performance and computational costs.

1. Introduction

Global warming and the shortage of energy resources have made energy management system (EMS) a hot topic in the energy sector [1]. Industries have realized that developing improved EMS can potentially improve energy monitoring and budgeting. Efficient energy planning is important to reduce energy costs and optimize energy usage [2]. Enabling technologies for EMS are smart meters that measure energy consumption, which facilitates energy management at the household or building level [3]. Data collected from smart meters are valuable assets for data-driven analytics and decision-making with essential use cases, including gaining insight into consumption trends, forecasting the energy consumption load, or optimizing energy exchanges in smart microgrids, which are all core functional building blocks for EMS [4].

Different prediction horizons are prominent in the load forecasting literature: short-, medium-, and long-term forecasts [5]. Short-term forecasts refer to a prediction horizon from a few minutes to days ahead. These forecasts are essential for decision-making that involves prosumers in smart energy grids [6]. Medium-term forecasts treat a horizon window of weeks to a few months, which is important for scheduling power systems [7]. Lastly, long-term forecasting refers to monthly or yearly predictions, which are utilized for the maintenance planning of the grid [8].

At the top level, load forecasting aims to predict the future demand for electricity load by end-use customers. Several methods can be used for load forecasting. Recently, machine learning (ML) methods have increased in popularity

✉ firas.bayram@kau.se (F. Bayram); phil.aupke@kau.se (P. Aupke); bestoun@kau.se (B.S. Ahmed); andreas.kassler@kau.se (A. Kassler); andreas.theocharis@kau.se (A. Theocharis); jonas.forsman@cgi.com (J. Forsman)
ORCID(s): 0000-0003-0683-2783 (F. Bayram); 0000-0001-9403-6175 (P. Aupke); 0000-0001-9051-7609 (B.S. Ahmed); 0000-0002-9446-8143 (A. Kassler)

[9] due to their simplicity of use. Having precise estimates of future energy demands would enable better decision-making [10] and more effective energy planning and scheduling strategies. However, load forecasting comes with challenges of its own. One major challenge is the changes in the patterns of energy consumption by consumers over time. These changes in patterns would cause a *concept drift* problem, which is induced by variation in the underlying statistical properties of the target variable [11]. This problem would lead to outdated ML models in the predictive system after the occurrence of the change [12].

There are many reasons to change the energy consumption behaviors of customers. For example, high or changing electricity prices have greatly impacted customer behavior [13]. Specifically, higher prices would cause what is known as *demand response*, which signifies that customers change their behavior in response to high prices [14]. Temporal or calendar factors such as year or type of day (e.g., weekday or weekend) are among the other sources of change in consumption behaviors, in addition to changes in the number of household members or the appliances used in the household [15]. Due to the dynamicity of the energy load consumption, the conventional ML paradigms do not perform well and suffer from performance degradation [16].

Considering the poor performance exhibited by classical ML solutions, deep learning-based approaches have been widely adopted in recent research on interval load forecasting since they achieve superior performance [17]. Specifically, Long Short-Term Memory (LSTM) is an effective algorithm that demonstrated high performance in the load forecasting problem [18]. Moreover, to maximize the efficiency of the deep learning (DL) models, an adaptive mechanism is fostered to cope with the changes in load consumption. This adaptation mechanism is set to automatically update the model and adjust it to the new energy usage pattern that presents concept drift [19]. In practice, concept drift is usually tracked actively or passively by the probability distribution that generates the data stream [20]. However, the main challenge in drift detection is determining a change magnitude threshold that exerts a great influence on overall predictive performance [21]. The change threshold should not be fixed, but should be tuned according to the present conditions of the system [22].

In this paper, we build an interval load forecasting learning framework based on dynamic drift adaptation for LSTM networks, namely DA-LSTM. We design different load forecasting solutions based on passive and active drift adaptation techniques. We highlight the advantages and disadvantages of each solution. Overall, the primary contributions and findings of this paper are summarized as follows:

1. A novel drift-adaptive LSTM (DA-LSTM) learning framework is proposed for interval load forecasting, which can be integrated with passive and active drift adaptation techniques.
2. A dynamic active drift detection methodology that identifies the change point in a consumer's behavior without fixing a drift magnitude threshold.
3. An adaptive LSTM network is designed to handle concept drift by quickly adapting to the new trend in load consumption while retaining the learned consumption patterns.
4. An extensive evaluation is conducted against baseline models from the literature to demonstrate the effectiveness of the proposed DA-LSTM framework.
5. A trade-off analysis between the different adaptation strategies is performed based on prediction performance and computational cost to suggest the adoption of the appropriate approach.

The remainder of the paper is organized as follows. In Section 2, we review the related work on load forecasting and Section 3 introduces the background of the problem. Section 4 introduces our novel drift-adaptive LSTM approach. Section 5 shows the experimental evaluation of our approach and demonstrates results, and Section 6 concludes the paper.

2. Related work

2.1. DL for Residential Load forecasting

The building characteristics and socio-economic variables are the most commonly used exogenous variables for building and occupancy prediction. Artificial neural network (ANN), bottom-up, time series analysis, regression, and Support Vector Machines (SVM) are the most often used load forecasting models, according to a survey by Kuster *et al.* [23]. The survey has also concluded that most regression models are used for long-term prediction, one year or more, while ML-based algorithms, such as ANN, especially DL, and Autoregressive Integrated Moving Average (ARIMA) [24], are commonly used for short-term prediction [25], which is also what we aim for. Alternative methods in the

literature consider additional variables to improve forecasting accuracy. For example, the model provided by Hong *et al.* [26] leverages iterative ResBlocks in a Deep Neural Network (DNN) to learn the spatial-temporal correlation among different types of user's electricity consumption habits.

DL algorithms such as Recurrent Neural Networks (RNNs) and Convolutional Neural Networks (CNN) have demonstrated significant efficiency. Nevertheless, these approaches use offline learning: they are taught only once and miss the potential to learn from newly arriving data. Sehovac *et al.* [27] proposed Sequence to Sequence Recurrent Neural Network (S2S RNN) with attention to load forecasting. The concept behind S2S RNN is based on adopting an attention mechanism [28], often utilized in language translation, to load forecasting to improve accuracy. The attention mechanism in the method is added to ease the connection between the encoder and decoder. A hybrid approach between RNN and Principal Component Analysis (PCA) technique has been proposed by Veeramsetty *et al.* [29] in a short-term load forecasting problem. The approach can capture the temporal resolution diversity using a heterogeneous input structure with PCA. The PCA-based summarized input features are used as input to an RNN model.

LSTM network is a particular type of RNN that has been effectively utilized in load forecasting problems. Zang *et al.* [30] have combined LSTM and attention mechanism for load forecasting of residential households. The approach constructs pools of users based on mutual information to increase the diversity of data used to train LSTM networks. To leverage the advantages of both networks, an integration between CNN and LSTM has been frequently used in the load forecasting literature [31, 32, 33, 34]. CNN exhibits high capabilities in feature learning, while LSTM can handle short- and long-term temporal dependencies between time steps. Additionally, recent studies have demonstrated the effectiveness of employing advanced neural networks for load forecasting such as temporal convolutional network (TCN) [35, 36], and Restricted Boltzmann Machine (RBM) [37]. However, changes in customer behaviors can lead to deterioration in the performance of the learning algorithm. Therefore, load forecasting approaches have been integrated with a drift-adaptive methodology to cope with the change [38].

2.2. Load Forecasting with Concept Drift

Only a few approaches have accommodated concept drift adaptation techniques in the load forecasting models. In recent studies, Fekri *et al.* [39] proposed an online adaptive RNN technique for load forecasting that considers concept drift. The model can learn and adapt to changing patterns as they emerge. This is done by adjusting the RNN weights online based on fresh data to retain time dependencies. The on-the-fly adjustment of the RNN parameters is activated in the event of performance degradation. Similarly, Jagait *et al.* [40] has proposed an adaptive online ensemble with RNN and ARIMA for load forecasting in the presence of concept drift. The adaptation to changes is made by adding Rolling ARIMA to the ensemble. Another approach that uses incremental ensemble learning has been presented in [41]. The model uses a heterogeneous learning process to build an ensemble that deals with seasonality and concept drift. Fenza *et al.* [42] presented a drift-aware solution to distinguish the anomaly behavior of customers from the regular pattern. The change is detected based on the standard deviation of the prediction error in the last week.

In a different approach proposed by Ji *et al.* [43], the ADaptive WINdowing (ADWIN) algorithm [44] has been utilized in short-term load forecasting problems to detect concept drift in a model updating method. Load forecasting methods that rely on calendar or weather information trained on historical data fail to capture significant break induced by lockdown and have performed poorly since the COVID-19 pandemic began. The article in [45] anticipates the electricity demand in France during the lockdown period, demonstrating its ability to significantly minimize prediction errors compared to conventional models. The method uses Kalman filters and generalized additive models to produce an accurate and rapid forecasting strategy to respond to the sudden shift in data. However, existing approaches that rely on drift adaptation require setting a drift threshold to trigger the alarm, which is a drawback, as it primarily influences predictive performance [21].

With the limited number of studies that exploit drift handling techniques in the load forecasting area, we propose a novel framework that combines drift adaptation approaches with LSTM networks. We incorporate a dynamic drift detection technique that does not require a pre-defined drift threshold into the framework. Instead, the method checks how extreme the drift magnitude is by leveraging the distribution of the drift magnitudes. In this way, there is no need to define a drift threshold that can be difficult to determine or fix throughout the learning process. Furthermore, the proposed framework can respond rapidly to drifts by taking advantage of the most recent patterns. At the same time, the framework can retain the learned knowledge, which may re-appear in the future. We performed extensive experimental analysis on a real-world energy consumption dataset. The result demonstrates the strength of our framework in prediction accuracy compared to traditional techniques.

3. Background

The statistical properties of the data streams often do not remain stable over time and changes are likely to occur, a phenomenon known as *concept drift* [46]. Statistical tests are usually used to monitor and detect concept drift. Concept drift typically leads to a reduction in the accuracy of forecasting models. Adaptation strategies have typically been implemented to cope with performance loss that update the models to cope with drift [47]. Concept drift adaptation strategies can be categorized into *passive*, also known as *blind*, and *active*, also known as *informed*, methods [48]. A passive adaptation denotes the drift adaptation that does not include drift detection techniques, and the predictor is regularly updated [49]. An active adaptation is the drift adaptation strategy that is actively triggered once a concept drift alarm is signaled from a concept drift detector [50].

In the load forecasting context, changes in consumption behavior may have multiple reasons, including changes in the number of household members, weather variations, or adding new electrical appliances and devices such as gaming PCs or electric vehicles. Thus, the concept drift solution strategy should be mainstreamed in load forecasting problems. This section summarizes the background on the change-point detection problem and the adaptive mechanism introduced in the LSTM network to cope with the drift.

3.1. Change-Point Detection

To identify variations in load consumption behavior, change-point detection methods are employed to test whether load consumption data have followed a change at a specific time point t . The following subsections present the definitions and notations for the change-point detection problem. We then illustrate the methods used to detect changes in load consumption patterns using distributional similarity measures.

3.1.1. Problem Formulation

Change-point detection, also known as *drift detection*, refers to the techniques used to identify change points of time-series data (such as electrical load) where a significant change has occurred in the underlying probability distribution that generates the data points [51]. The change detectors are usually coupled with a predictive system. When the change exceeds the significance level, the detectors signal an alarm and evoke the learner to be updated or replaced in the forecasting system [52]. Practically, the change signal is delayed by at least one time point [48]. The mechanism of change-point detection algorithms is illustrated in Fig. 1. Different performance indicators for the change-point detection algorithms are annotated in the figure. For example, the detection delay δt is the time between drift occurrence and detection. Another indicator is the misdetection rate, which quantifies the number of changes missed by the algorithm. In contrast, the false alarm rate is the ratio of incorrectly detected change points compared to real drift occurrences. However, in real-world datasets, the ground-truth information of changes is usually indeterminate [53]. Therefore, the performance of change-point detection methods is usually assessed by the predictive performance of the ML model along with the associated adaptation costs.

In load forecasting problems, data are typically recorded as time-series vectors, and it is fundamental to divide these data vectors into time-series samples for the purpose of drift detection. Analogously to the formulation presented by Liu *et al.* [51], we define the following notation of our problem. Let $\mathbf{Y}(t) \in \mathbb{R}^k$ be a sequence of univariate time series of load consumption observations with length k at time t :

$$\mathbf{Y}(t) := [y(t-k+1), \dots, y(t-1), y(t)]^\top \in \mathbb{R}^k,$$

where $y(t) \in \mathbb{R}$ is a single load consumption observation with an order that signifies the temporal dependency between the observations of each time-series sequence, $^\top$ denotes the transpose operation of the vector. By convention, since the granularity of the change-point detection analysis of time-series data is the entire sequence of load consumption observations $\mathbf{Y}(t)$ rather than a single observation $y(t)$, the term “*sample*” is adopted to refer to the overall sequence of observations $\mathbf{Y}(t)$, instead of the single observation $y(t)$ [54, 51]. Therefore, the set of n consecutive load consumption samples at time t is defined as:

$\mathbb{Y}(t) := \{\mathbf{Y}(t-n+1), \dots, \mathbf{Y}(t-1), \mathbf{Y}(t)\}$. The task of change-point detection is to identify the (dis)similarity between two samples at time t . Typically, the (dis)similarity score $D(t)$ is calculated using the probability distributions of the two samples. This similarity score will be used as an indicator to diagnose the status of the time-series data. In load forecasting literature, existing methods that employ drift detectors compares $D(t)$ to a pre-defined threshold λ to detect change points [55, 56]. However, energy consumption patterns are characterized by high volatility [57]. Therefore, the threshold λ must be dynamic to cope with the changing nature of the energy consumption patterns.

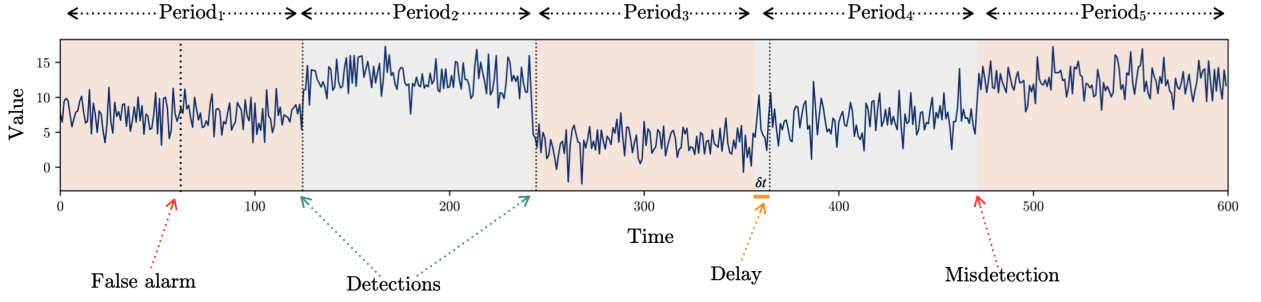


Figure 1: Change-point detection in time-series data

3.1.2. Divergence-Based Similarity Score

As defined in Section 3.1.1, change-point detection methods rely on identifying the significance of the change incurred in the data-generating probability distributions. A prevalent approach to measure the similarity between two or more probability distributions of load consumption data is to calculate the divergence between these distributions [58]. Higher magnitudes of the divergence values indicate a more significant dissimilarity between probability distributions.

In our settings, we are interested in measuring the similarity at time t between the probability distribution of two consecutive samples of load consumption data to inspect the drift at t . The similarity score $D(t)$ will be calculated based on the comparison between a reference sample of load consumption $\mathbf{Y}_{rf} = \mathbf{Y}(t-1)$ and the most recent sample of load consumption in which the similarity will be tested $\mathbf{Y}_{ts} = \mathbf{Y}(t)$. Note here that the samples are set to be segmented according to a pre-defined window size. Windowing techniques generally require defining the window size based on the number of data points or the time interval [59]. The selection of window size will be explained in Section 4.1.

Jensen-Shannon divergence (JSD) is one of the most popular metrics used to measure the magnitude of the distributional change that the time-series data have followed at a specific time point t [60]. JSD is a well-grounded symmetrization of the well-known Kullback–Leibler Divergence (KLD) metric. Liu *et al.* [51] showed that using a symmetric divergence metric leads to greater change-point detection performance. The distance between two probability distributions using JSD is defined as [61]:

$$\text{JSD}(P_{rf} \| P_{ts}) = \text{JSD}(P_{ts} \| P_{rf}) := \frac{1}{2} \left(\text{KL} \left(p_{rf} \| \frac{p_{rf} + p_{ts}}{2} \right) + \text{KL} \left(p_{ts} \| \frac{p_{rf} + p_{ts}}{2} \right) \right), \quad (1)$$

where P_{rf} and P_{ts} are the probability distributions for the reference and test samples \mathbf{Y}_{rf} and \mathbf{Y}_{ts} , respectively, the function KL represents KLD and is given by:

$$\text{KL}(P \| Q) := \int p(\mathbf{Y}) \log \left(\frac{p(\mathbf{Y})}{q(\mathbf{Y})} \right) d\mathbf{Y}. \quad (2)$$

Therefore, JSD can be written as:

$$\text{JSD}(P_{rf} \| P_{ts}) = \text{JSD}(P_{ts} \| P_{rf}) := H \left(\frac{p_{rf} + p_{ts}}{2} \right) - \frac{H(p_{rf}) + H(p_{ts})}{2}, \quad (3)$$

where the function H denotes Shannon's entropy:

$$H(p) = - \int p(\mathbf{Y}) \log p(\mathbf{Y}) d\mathbf{Y}. \quad (4)$$

In addition to its symmetry, JSD exhibits several pertinent properties: It is always defined and bounded in the interval $[0, 1]$ for two probability distributions, while the value of KLD can diverge to infinity and can take values in the interval $[0, \infty)$, and the square root of JSD satisfies the triangle inequality [60]. For the abovementioned properties, we use the square root of JSD as the distance metric in the change-point detection experiments.

3.1.3. Nonparametric Density Estimation

Density estimation is the technique used to recover the probability density function that generates the dataset. As we can see from Eq. 3, to calculate the JSD value we first need to find the probability distribution $p(\mathbf{Y})$ to determine the distance between the samples. Several methods to estimate the probability distribution can be found in the literature. Histograms and Kernel Density Estimation (KDE) methods are the most widely used nonparametric approaches to reconstruct the underlying probability density function using a given dataset.

Although, in general, KDE has a slower convergence rate of magnitude N^{-1} than traditional histograms [62], where N is the number of data points, histograms are susceptible to exhibit a lower convergence rate in dynamic environments that are characterized by changing variance. When the dispersion of the data changes, the number of bins should be varied as suggested by [63, 62]. However, KDE suffers from the so-called phenomenon *curse of dimensionality*, which makes the convergence rate very slow when the dimension of the problem is large [64]. The optimal convergence rate of KDE is $O\left(N^{-\frac{2}{d+4}}\right)$, where d is the dimension of the data. We have adopted the KDE method in estimating the density because this phenomenon will not affect the performance of our proposed solution since the time-series samples of our dataset are *univariate*.

To produce the density profile, KDE places a kernel at each data point y_i , and then sums these individual kernels together to obtain the final density estimate. This method will render a smooth curve, which is one of the salient advantages of the KDE method [65]. At regions with a high density of data points, the KDE will yield a large value, because many points will contribute to the sum value. However, it will yield a low value for regions with only a few data points. With (y_1, y_2, \dots, y_n) being a sample of n observations whose underlying probability distribution is to be estimated, where $y_i \in \mathbb{R}^d$. The standard KDE function is formally expressed as follows [66]:

$$\hat{p}_n(y) = \frac{1}{nh^d} \sum_{i=1}^n K\left(\frac{y - Y_i}{h}\right), \quad (5)$$

where K is a smooth kernel function $K : \mathbb{R}^d \mapsto \mathbb{R}$, $h > 0$ is the bandwidth or the smoothing parameter. As has been remarked in the literature, the choice of the kernel function is not instrumental for KDE [67], and the difference in the estimation error is considered negligible [64]. Thus, for selecting the kernel function, we opted to use the Gaussian kernel, which is the most common kernel function, given by the form:

$$K\left(\frac{y - Y_i}{h}\right) = \frac{1}{\sqrt{2\pi}} e^{-\frac{(y-Y_i)^2}{2h^2}}. \quad (6)$$

On the contrary, as can be noticed in Eq. 5, the density function is strongly affected by the selection of the bandwidth parameter. Therefore, different bandwidth values would give different density function values as it controls the *smoothness* or *roughness* of the density estimate (see Eq. 6). Many procedures attempt to adaptively determine the optimal bandwidth parameter [68], mainly by minimizing the asymptotic mean integrated square error (AMISE) estimations of KDE [69]. The drawback of such automated procedures for adaptive smoothing would most likely lead to the selection of different values of bandwidth parameters for different samples. This means that the amount of smoothing varies between different time intervals or households in our problem, and thus the comparison between the data distributions is incoherent. In this case, the divergence calculation would be futile because the densities are constructed with different amounts of smoothing. To overcome this drawback, we have used a fixed bandwidth value across all the samples to extract homogeneous KDE functions and make the distance calculation valid. Conventionally, bandwidth is set according to domain expertise for load forecasting and is customized for the specific problem using data-driven statistics [70]. In this paper, we have set the bandwidth value to **10** based on empirical experience gained from observing the standard deviation of the load consumption across all customers.

3.2. Conventional LSTM

The conventional LSTM [71] is a sort of RNN but with additional long-term memory. The standard RNNs uses recurrent cells such as sigma, which can be expressed as follows [72]:

$$\begin{aligned} h_t &= \sigma(W_h h_{t-1} + W_x x_t + b), \\ y_t &= h_{t+}, \end{aligned} \quad (7)$$

where x_t , h_t and y_t represent the input, recurrent information, and the output of the cell at time t , respectively, W_h and W_x are the weights, and b is the bias. The time-series sample for x_t and y_t are derived from $\mathbf{Y}(t)$. Although the usage of standard RNNs cells provided success in problems such as sentiment analysis or image classification ([73],[74]), they typically cannot treat long-term dependencies well. LSTM networks can remember values from earlier stages to use in the future, which deals with the vanishing gradient problem [75]. This problem occurs because the network cannot backpropagate the gradient information to the input layers of the model due to activation functions. The sigmoid function, for example, normalizes large input values in a space between 0 and 1. Therefore, a large change in the input will cause a small change in the output. Therefore, the derivative becomes small and possibly vanishes [76]. To deal with this problem, [75] introduced gates into the cell.

The conventional LSTM cell features three gates (input, forget, and output), a cell, block input, and an output activation function. The cell output is recurrently connected back to the cell input and all the gates. The forget gate was not part of the initial LSTM network, but was proposed by Gers *et al.* [77] to allow the LSTM to reset its state. The three gates regulate the flow of information associated with the cell.

The input gate combines the current input X_t , the output of the prior LSTM cell $h_{(t-1)}$ and the cell state $C_{(t-1)}$. The following equation illustrates the procedure [72]:

$$i^{(t)} = \sigma (W_i x^{(t)} + R_i h^{(t-1)} + p_i \odot c^{(t-1)} + b_i), \quad (8)$$

where \odot denotes point-wise multiplication of two vectors, W_i , R_i , and p_i are the weights associated with x_t , $h_{(t-1)}$, and $C_{(t-1)}$, respectively. b_i represents the bias vector associated with this component. The prior LSTM layer determines which information should be retained in the cell states c_t . This includes the selection of candidate values z_t that could be added to cell states and activation values i_t of the input gates.

The forget gate determines which information should be removed from its previous cell states $C_{(t-1)}$. Therefore, the activation values f_t are calculated based on the current input x_t , the outputs $h_{(t-1)}$ and the state $C_{(t-1)}$ of the memory cells at the previous time step ($t - 1$).

$$f^{(t)} = \sigma (W_f x^{(t)} + R_f y^{(t-1)} + p_f \odot c^{(t-1)} + b_f), \quad (9)$$

where W_f , R_f , and p_f are the weights associated with x_t , $h_{(t-1)}$ and $C_{(t-1)}$, respectively, while b_f denotes the bias vector.

The cell state combines the input values of the block z_t , the input gate i_t , and the forget gate f_t , with the previous cell value:

$$c^{(t)} = z^{(t)} \odot i^{(t)} + c^{(t-1)} \odot f^{(t)}. \quad (10)$$

The output gate combines the current input x_t , the output of the previous unit $h_{(t-1)}$, and the cell value $C_{(t-1)}$ in the last iteration:

$$o^{(t)} = \sigma (W_o x^{(t)} + R_o h^{(t-1)} + p_o \odot c^{(t)} + b_o), \quad (11)$$

where W_o , R_o and p_o are the weights associated with x_t , $h_{(t-1)}$ and $C_{(t-1)}$, respectively, while b_o denotes the bias weight vector.

3.3. Adaptive LSTM

Inspired by incremental learning techniques, which are useful in solving drift problems [78], we continuously adapt the LSTM model to pertain to the previously acquired knowledge and update the model based on the most recent data that represent the current trend in load consumption. Incremental learning is an ML paradigm in which the learning process continually evolves whenever new samples emerge. Furthermore, incremental learning adjusts what has been learned according to these newly available samples [79]. The literature provides different definitions for incremental learning ([80, 81, 82, 83]). In this paper, we adopt a universally accepted setting for incremental learning that satisfies the following conditions ([82, 83]):

- Knowledge obtained previously should be preserved;
- Learning new knowledge from new data should be possible;

Table 1
Search space for hyperparameter values

Hyperparameter	Values
Learning rate	LR=[0.0001, 0.001, 0.01]
Dropout rate	DR=[0, 0.1, 0.5]
Number of units in the LSTM layer	$N_U=(32: 32: 512)$

Algorithm 1 Bayesian Hyperparameter Optimization

```

1:  $P_{model} \leftarrow Surrogate(f(x))$ 
2:  $x_{\star} \leftarrow []$ 
3: while  $i < maxIterations$  do
4:    $x_{\star} \leftarrow P_{model}(score, hyperparameters)$ 
5:    $score \leftarrow f(x_{\star})$ 
6:    $P_{model} \leftarrow Update(P_{model}, score)$ 
7: end while

```

- Knowledge of previous historical data is not required when updating the model;
- Changes in the characteristics of the new data should be learned.

Incremental learning algorithms can be categorized into two main approaches: the growing or pruning of the model architectures [84] and the controlled modification of the learner weights [85, 86]. In this paper, we adopt the latter approach, which is appropriate for load forecasting tasks. The main motivation for our choice is that old consumption behavior usually reoccurs in the future due to seasonality [87]. Therefore, modifying the current models while preserving the previously learned knowledge would be more favorable than completely forgetting the historical knowledge. The adaptation is divided into two main steps: the hyperparameter optimization (HPO) technique and the adaptation of the LSTM model.

3.3.1. Hyperparameter Optimization (HPO)

HPO is a technique to find the best combination of hyperparameters that optimize the performance of ML model [88]. Tuning the hyperparameters for specific problems leads to increased performance [89].

Different techniques are used in the literature to automatically find the optimal hyperparameters. Grid search and random search are the most basic HPO methods. However, they suffer from unawareness of past evaluations, which often leads towards sub-optimal hyperparameters [90]. Bayesian optimization (BO) [91] overcomes this by keeping track of previous evaluations by forming surrogate models to map hyperparameters to a probability P of the objective function score:

$$P(\text{score} \mid \text{hyperparameters}). \quad (12)$$

BO uses probabilistic surrogate models for the objective function because they are easier to optimize than the actual objective function. The process of BO is described in Algorithm 1. The probabilistic model P_{model} is initialized on $f(\cdot)$ a priori. For each iteration, the best set of x_{\star} is found for the current P_{model} model, and the model $score$ for the set x_{\star} is determined and P_{model} is updated [91].

Since we apply incremental learning techniques in this work, using HPO for every hyperparameter available in LSTM networks is not applicable. Structural hyperparameters, such as the number of layers and the size of the hidden layer affect the weights of the model. Changing those requires a complete retraining of the surrogate model, which invalidates the purpose of surrogate models, in general. However, non-structural hyperparameters such as learning and dropout rate do not require a complete re-training of the model, which makes their tuning applicable in this case [39, 92]. Table 1 illustrates the ranges of the non-structural hyperparameters used for the HPO in the experiments.

3.3.2. Adaptation of LSTM Model

As mentioned above, we were inspired by incremental learning techniques to adapt the LSTM model. To suit the receiving data for the model, we followed the batch-wise approach for incremental LSTM used in [93]. Since LSTM expects the dataset as batches for the training, we divide it into multiple sub-batches for incremental processing.

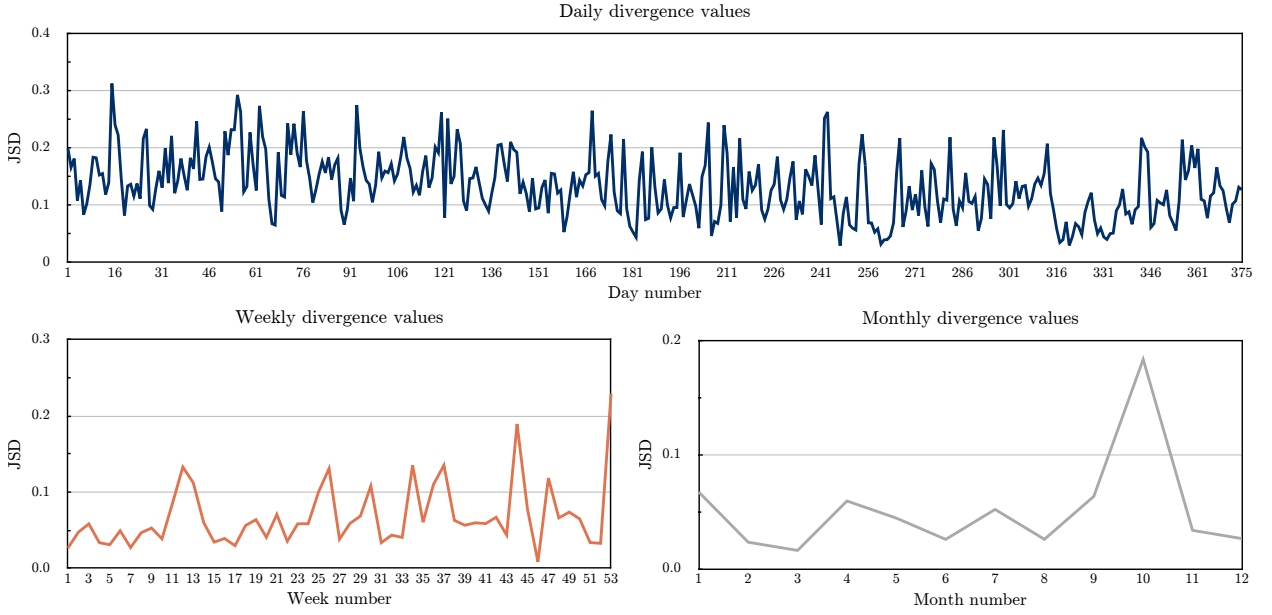


Figure 2: JSD divergence magnitude using different temporal granularity levels for the households

The stored weights W_t of the baseline model LSTM retain the knowledge preserved from the previous historical data. After an update signal is triggered, these weights must be adapted to the new batch of data points and the corresponding updated non-structural hyperparameters. To preserve already learned knowledge and reduce training time, stored weights W_t are updated only with new data points, excluding previous historical data. This is enabled by the possibility of continuing the training at the point of the storage of the weights W_t . The new weights $W_{(t+1)}$ of the adapted model are stored later to be used for the next update signal.

4. Proposed Drift-Adaptive LSTM (DA-LSTM)

The LSTM algorithm was integrated into a drift-adaptive learning framework using adaptation techniques. The techniques are active and passive approaches based on the methodology implemented to trigger the adaptation of LSTM networks. This section explains the selection of drift detection granularity and the drift-adaptive LSTM (DA-LSTM) approaches.

4.1. Drift Adaptation Granularity

As discussed in Section 3.1, change-point detection requires comparing the distributions of different samples. The samples should be partitioned according to a specific windowing strategy. Therefore, the data distribution is built for these windows. The main ingredient for such windowing strategies is the window size that represents the checking points to monitor the drift occurrence. The selection of window size significantly affects drift analysis and should be carefully decided [94]. In load forecasting, the load consumption trends can be monitored across spatial or temporal scales [95]. But since our dataset, as will be discussed in Section 5.1, does not have spatial information about the households, we have used temporal granularity to divide the time-series data.

Different levels of granularity can be defined to check the efficacy of the adaptation methods. For good performance, it is important to determine the optimal temporal granularity for drift analysis. Short-term forecasting was shown to deliver the best performance among prediction horizons [96]. To support this argument, we have compared the drift magnitude for the household consumption data according to different temporal granularity levels: daily, weekly, and monthly. The JSD values of all customers are averaged, and the results are reported in Fig. 2. As we can see, the daily granularity shows the highest level of drift magnitude by showing the most significant divergence values. For this reason and to avoid overriding drift occurrences, we have adopted daily granularity in our adaptation solution.

Algorithm 2 Passive drift adaptation algorithm**Input:** Historical time-series samples $\mathbb{Y}(t-1)$ **Output:** Learner $f^{(t)}$

- 1: **Initialize:** $f^{(t-1)}(\mathbb{Y}(t-1))$
- 2: **for** $\mathbf{Y}(t), t = 2, \dots$ **do**
- 3: Update $f^{(t)} \leftarrow f^{(t-1)}(\mathbf{Y}(t))$
- 4: Predict $f^{(t)}(\mathbf{Y}(t+1))$
- 5: Calculate E_{t+1}
- 6: **end for**

4.2. Passive Adaptation Approach

The passive drift adaptation scheme is similar to incremental learning from a technical point of view [97]. The primary analogy is that both mechanisms work without explicitly detecting a change, i.e., no drift detector component is involved, and the learning process evolves with the data arrival. Following the integration of this adaptation mechanism with the learning process, the model is updated after a specific time interval or chunk size. This periodicity is identified to sufficiently resemble the latest consumption trend and thus can handle the potential change in the time series.

Algorithm 2 outlines the passive drift adaptation approach, which periodically updates the LSTM networks. The periodicity of the model update assumes a *daily* granularity, as it shows the highest drift significance, as discussed in Section 4.1. First, the LSTM model is initialized using the historical time-series data. A daily update signal is sent to the LSTM model to be updated according to the method explained in Section 3.3. This update mechanism is designed to incorporate the most recent consumption trends represented by the most recent data.

However, one of the criticisms of this approach is derived from the constant update of the trained learner. This setup of constant updates might accommodate unnecessary updates when the time-series data have been stationary in some intervals. The unnecessary updates would cause an avoidable computational cost and resources [98]. To overcome this drawback, we present an active approach, discussed in the next section, that only updates the model after drift detection in the time-series data.

4.3. Active Adaptation Approach

Drift detectors form the foundation of active adaptation solutions. The detectors continuously monitor the time-series data and perform a set of statistical tests to identify the changes in the data. In this approach, we employ a change-point detection based on Jensen-Shannon divergence to trace the changes in the time-series data distribution, see Section 3.1. Once the change exceeds a certain significance level τ , the adaptation phase is activated by sending an update signal to the LSTM networks. The LSTM adaptation is carried out as specified in Section 3.3.

One of the main challenges to create a drift detection method is selecting a suitable drift threshold [99]. Setting a low drift magnitude threshold would lead to an increased false alarm rate. However, setting a high threshold value would cause drift misdetections. In a recent study [22], the authors pointed out that the selection of a suitable drift threshold could have a greater impact on performance than the detection algorithm. Moreover, the authors have demonstrated that the drift threshold should not be fixed throughout the learning process and must follow the dynamicity of the data based on the current conditions. Motivated by these observations, we have developed a dynamic mechanism to efficiently signal a time-series data distribution change.

Algorithm 3 outlines our active drift adaptation approach. The algorithm first checks for drift occurrence and then makes predictions according to the drift analysis. We have developed the drift detection method based on monitoring the distribution of the divergence values calculated for each time window frame. The time window size is segmented according to the daily granularity as explained in Section 4.1. As detailed in lines 3-6 of Algorithm 3 and shown in Fig. 3, after each time window frame, the divergence $Div_t = JSD_t(P_{rf} \| P_{ts})$ is calculated between the probability density function of this specific day d at time t that represent the test samples PDF_{ts} and probability density function of historical data of all days that precede t which represent the reference samples PDF_{rf} , and so on. The divergence values are found using the Jensen-Shannon method (see Section 3.1.2), and the divergence metric is calculated on the densities that are estimated using the KDE methods (see Section 3.1.3). For a training dataset of length d periods that represent the temporal granularity of the drift detection mechanism, i.e., days in our case, $d-1$ divergence values are calculated that comprise the historical trends of changes in load consumption. These values will initialize the distribution of the divergence values before sliding on the evaluation dataset.

Algorithm 3 Active drift adaptation algorithm

Input: Historical time-series samples $\mathbb{Y}(t-1)$, probability distribution of historical divergence values $PDF(div_t)$, significance level τ

Output: Learner $f^{(t)}$, $PDF(div_{t+1})$

- 1: **Initialize:** $f^{(t-1)}(\mathbb{Y}(t-1))$
- 2: **for** $\mathbf{Y}(t)$, $t = 2, \dots$ **do**
- 3: Calculate $PDF(\mathbf{Y}(t)) \leftarrow KDE(\mathbf{Y}(t))$
- 4: Calculate $PDF(\mathbb{Y}(t-1)) \leftarrow KDE(\mathbb{Y}(t-1))$
- 5: Calculate $Div_{t+1} \leftarrow JSD(PDF(\mathbf{Y}(t)) || PDF(\mathbb{Y}(t-1)))$
- 6: Calculate $PV(div_{t+1}) \leftarrow P\text{-value}(PDF(div_t), Div_{t+1})$
- 7: **if** $PV(div_{t+1}) < \tau$ **then**
- 8: Update $f^{(t)} \leftarrow f^{(t-1)}(\mathbf{Y}(t))$
- 9: Predict $f^{(t)}(\mathbf{Y}(t+1))$
- 10: **else**
- 11: Predict $f^{(t-1)}(\mathbf{Y}(t+1))$
- 12: **end if**
- 13: Calculate E_{t+1}
- 14: **end for**
- 15: Update $PDF(div_{t+1}) \leftarrow [PDF(div_t), div_{t+1}]$

After the initialization step, the divergence-based similarity score is found using the sliding window mechanism for each temporal granularity frame of the evaluation samples. Then, we test the null hypothesis of no change in the time-series data. The algorithm checks the p-value of the observed divergence value associated with the historical divergence value distribution. As illustrated in Fig. 4, the algorithm rejects the null hypothesis if the value exceeds the significance level τ and assumes a change in the behavior of the consumption load. The p-value is equal to the area under the curve of the probability density function [100]. Our approach is dynamic for detecting the change point without fixing a detection threshold. This happens because the distribution of the divergence values evolves with the recording of more observations for load consumption. Furthermore, the significance level τ represents how extreme the divergence can be before signaling a change. The main advantage of using the p-value is that it is more persistent than a threshold that could be volatile for the change detection problem; hence, it is a more reliable indicator. The significance level τ controls the sensitivity to detect changes regardless of the magnitude of this change measured by the divergence metric.

5. Experimental Evaluation and Results

The performance of the ML predictions is evaluated using energy consumption records from real-world datasets that include nine households. However, for more detailed evaluations, we specifically selected two example households, namely Household 1 (an apartment) and Household 7 (a house). These households were chosen because they represent different types of households, allowing us to assess the performance of our model under varying conditions. The performance of ML predictions is affected by the detection of and reaction to drifts. Typically, drift adaptations improve the model's accuracy by performing a retraining or update process, which may impact the computational cost. Therefore, there is a trade-off between prediction accuracy and computational cost.

In this section, we answer the following questions:

- **Prediction performance (Section 5.3):** How accurately do active and passive DA-LSTMs predict the energy demand for different parameters?
- **Computational Cost (Section 5.4):** What is the impact on the computational cost of both active and passive approaches?
- **Performance-cost trade-off (Section 5.5):** What is the trade-off between performance and cost, and how can we use it to select the most suitable approach?

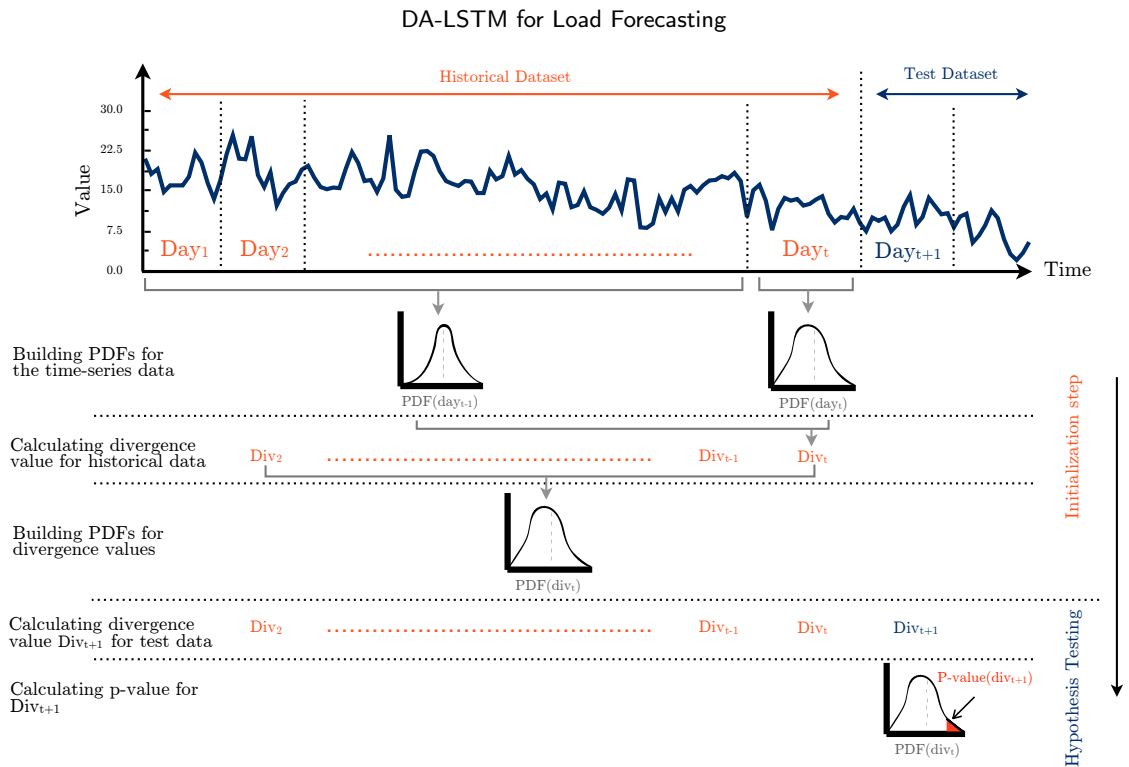


Figure 3: Active detection method based on dynamic drift magnitude

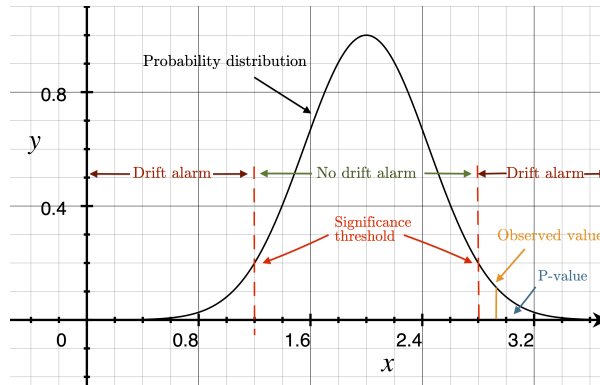


Figure 4: Drift alarms based on hypothesis testing

- **Real-life Pros and Cons (Section 5.6):** What are the advantages and disadvantages of each approach in real-life problems?

5.1. Consumption Dataset

To evaluate our approach, we used consumption data from the Swedish Energy Agency or Energimyndigheten¹. It contains the energy consumption of nine customers for one year at a resolution of ten minutes. Detailed information on the dataset is shown in Table 2. The table presents the start and end dates for the training and test dataset, divided by 75% and 25%, respectively. We chose this split since it showed a better prediction performance for datasets that are affected by seasonality [101]. The validation dataset was created with $\frac{1}{6}$ of the entire training dataset for each customer, allowing for a reasonable amount of data to be used for training while still reserving a portion for validation

¹<https://www.energimyndigheten.se/>

Table 2
Information of energy consumption dataset

Household information		Training and validation dataset			Test dataset		
Household	Type	Start date	End date	Size	Start date	End date	Size
Household 1	Apartment	18.08.2005	24.06.2006	44640	24.06.2006	23.08.2006	8640
Household 2	Apartment	24.12.2005	08.01.2007	42768	08.01.2007	22.03.2007	10512
Household 3	Apartment	22.03.2006	29.01.2007	44640	29.01.2007	30.03.2007	8640
Household 4	Apartment	24.04.2007	08.03.2008	44640	08.03.2008	07.05.2008	8640
Household 5	Apartment	21.08.2005	05.07.2006	44496	05.07.2006	04.09.2006	8784
Household 6	Apartment	02.09.2005	07.07.2006	44784	07.07.2006	04.09.2006	8496
Household 7	House	01.09.2005	30.07.2006	44064	30.07.2006	02.10.2006	9216
Household 8	House	15.09.2005	28.07.2006	44496	28.07.2006	27.09.2006	8784
Household 9	House	04.10.2006	15.08.2007	44496	15.08.2007	15.10.2007	8784

and effectively capturing the complexity of the data. Additionally, information on the type of housing is given.

5.2. Experimental setup

5.2.1. Baseline Methods

To establish a comparable basis for the evaluation, we trained a baseline LSTM model and several baseline methods that are frequently used in load forecasting problems for each household individually. In particular, the baseline methods are: LSTM, Rolling ARIMA, Bagging Regression [102] and an RNN model [103, 40]. For LSTM-based methods, the structure of the model consists of a singular LSTM layer combined with a dense layer. For each model, we individually tune the hyperparameters. The dataset of each household was divided into training and test sets according to the specifications mentioned in Section 5.1. Each of the predictors takes 12 time steps (2 hours) as input and generates a prediction for the next six time steps, equal to an hour ahead. In addition, we created an LSTM model for the passive and active approaches, respectively.

5.2.2. Evaluation Parameters

For the active drift detection approach, three significance levels of p-values are defined: 0.07, 0.10, and 0.15. The significance level controls the extremeness of change magnitude for flagging a drift alarm. The higher the level value, the more probable the null hypotheses will be rejected because more values will fall within the drift-alarm region. The passive approach is equivalent to setting the p-value significance level to 1, meaning a drift always occurs. On the contrary, the baseline approach is equivalent to setting the p-value significance level to 0, i.e. a drift never occurs.

5.2.3. Error Metrics

To measure the prediction performance, we used Mean Absolute Percentage Error (MAPE) and Root Mean Square Error (RMSE) as evaluation metrics since they are the most common error metrics used in the load forecasting literature according to a survey by Nti *et al.* [104]. To compare the results daily, we take the mean of 24 prediction errors as we detect changes on a daily basis. Since we predict an hour in advance, we calculate the mean of error metrics of 24 predictions for each day as follows:

$$\text{MAPE} = \frac{1}{n} \sum_{t=1}^n \left| \frac{A_t - F_t}{A_t} \right| * 100, \quad (13)$$

$$\text{RMSE} = \sqrt{\frac{1}{n} \sum_{t=1}^n (A_t - F_t)^2}, \quad (14)$$

where A_t represents the vector of the actual consumed energy, F_t the forecasted ones and n is the number of predictions.

5.2.4. Computing Environments

To gain insight into the operational efficiency of each approach, we deploy the solution on Amazon Web Services (AWS)² cloud service. This will facilitate the trade-off analysis between the prediction performance and computational

²<https://aws.amazon.com/>

Table 3
Computational specifications

Local Environment	
CPU	Intel Core i9-9900X CPU, 20 Threads
GPU	Nvidia GeForce RTX 2080, 11GB GDDR6
RAM	64GB DDR4
AWS	
CPU	Intel Xeon Scalable Processors, 16 Threads
GPU	Nvidia T4, 16GB GDDR6
RAM	64GB DDR4

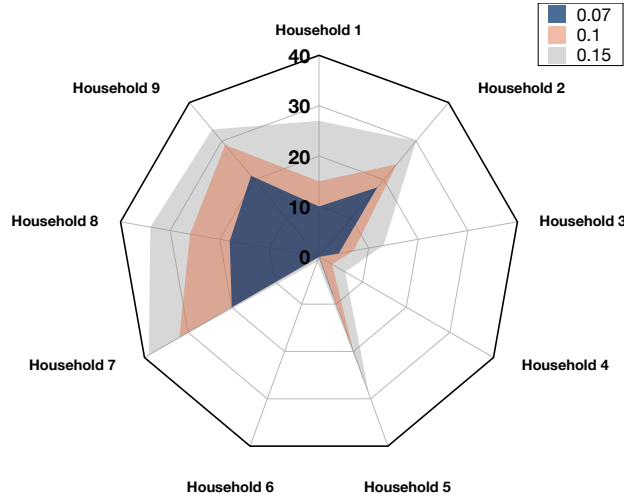


Figure 5: Detection counts per household for active approaches with different significance values τ

cost. AWS is one of the most popular public-cloud providers and frequently used as a deployment service for AI applications [105]. To quantify the computational cost, we measure the usage of Central Processing Unit (CPU) and Graphics Processing Unit (GPU) during run-time and the costs of running the approaches in a cloud environment (AWS). Table 3 presents the specifications for the local machine and the corresponding AWS instance. We selected a G4 instance, namely: g4dn.4xlarge³. For the calculation of the computational cost of the AWS instance, we measured the training time for the adaptation and calculated the on-demand price of the instance for that period, similar to [106].

5.3. Prediction Performance of DA-LSTM

We conducted an exhaustive performance evaluation of our proposed DA-LSTM method against a conventional LSTM model, as it represents the main benchmark for comparison. Furthermore, we compared our method with several other baseline methods in the literature. However, we performed a more exhaustive evaluation for the conventional LSTM model, given that our proposed method is an improvement over it.

5.3.1. Comparison Against Conventional LSTM

The predictive performance of the different DA-LSTM strategies is evaluated and compared with the conventional baseline LSTM. We have also analyzed the drift detection counts for the active-based drift detection approach. The detection counts of all households with respect to the significance level value τ are summarized in Fig. 5. We can see that households of the type *House* have more irregular consumption patterns. Furthermore, some households do not have drift detected for a significance level of small values. This means that no adaptations are implemented for this household in the corresponding significance levels for the active approach.

Table 4 shows the prediction error of all households observed for passive and active approaches for different parameters. For each household, we calculate the overall mean MAPE, RMSE performance metrics, and the standard

³AWS instance: <https://aws.amazon.com/ec2/instance-types/g4/>

Table 4
MAPE performance results of all households

Household	Baseline LSTM		Active LSTM, $\tau = 0.07$			Active LSTM, $\tau = 0.1$			Active LSTM, $\tau = 0.15$			Passive LSTM		
	Mean	STD	Mean	STD	Imp	Mean	STD	Imp	Mean	STD	Imp	Mean	STD	Imp
Household 1	6.56	1.10	4.74	0.87	27.74 %	3.70	0.70	43.60 %	3.22	0.68	50.91 %	2.95	0.68	55.03 %
Household 2	4.05	2.85	4.03	0.85	0.49 %	4.02	0.79	0.74 %	3.50	0.73	13.58 %	2.53	0.16	37.53 %
Household 3	21.69	13.43	21.41	9.11	1.29 %	21.23	8.56	2.12 %	19.46	7.98	10.28 %	11.24	7.66	48.18 %
Household 4	9.48	9.18	9.48	0.00	0.00 %	6.54	0.93	31.01 %	5.55	0.51	41.46 %	5.10	0.18	46.20 %
Household 5	3.09	3.46	3.09	0.00	0.00 %	2.76	0.69	10.68 %	2.75	0.53	11.00 %	2.66	0.35	13.92 %
Household 6	4.34	3.64	4.34	0.00	0.00 %	4.34	0.00	0.00 %	3.59	0.24	17.28 %	2.62	0.06	39.63 %
Household 7	8.32	2.08	6.03	1.62	27.52 %	4.80	1.36	42.31 %	3.94	1.16	52.64 %	4.09	1.65	50.84 %
Household 8	6.11	7.85	6.01	1.68	1.64 %	6.01	1.45	1.64 %	5.43	1.02	11.13 %	5.33	0.68	12.77 %
Household 9	8.34	4.51	7.25	3.49	13.07 %	7.16	2.98	14.15 %	6.96	2.56	16.55 %	3.0	0.54	64.03 %
Average	8.00	5.34	7.36	2.04	8.62 %	6.73	1.94	16.25 %	6.04	1.71	24.98 %	4.39	1.33	40.90 %

Table 5
RMSE performance results of all households

Household	Baseline LSTM		Active LSTM, $\tau = 0.07$			Active LSTM, $\tau = 0.1$			Active LSTM, $\tau = 0.15$			Passive LSTM		
	Mean	STD	Mean	STD	Imp	Mean	STD	Imp	Mean	STD	Imp	Mean	STD	Imp
Household 1	0.45	0.15	0.32	0.08	28.88 %	0.25	0.07	44.44 %	0.23	0.06	48.88 %	0.21	0.07	53.33 %
Household 2	0.24	0.17	0.21	0.07	12.50 %	0.18	0.08	25.00 %	0.13	0.07	45.83 %	0.10	0.06	58.33 %
Household 3	0.74	0.25	0.52	0.17	29.72 %	0.45	0.15	39.18 %	0.39	0.10	47.29 %	0.32	0.08	56.75 %
Household 4	0.21	0.11	0.21	0.00	0.00 %	0.15	0.07	28.57 %	0.12	0.07	42.85 %	0.11	0.05	47.61 %
Household 5	0.19	0.10	0.19	0.00	0.00 %	0.12	0.08	36.84 %	0.10	0.06	47.36 %	0.08	0.06	57.89 %
Household 6	0.24	0.14	0.24	0.00	0.00 %	0.24	0.00	0.00 %	0.16	0.05	33.33 %	0.15	0.04	37.50 %
Household 7	0.42	0.19	0.25	0.10	40.47 %	0.19	0.08	54.76 %	0.18	0.07	55.89 %	0.18	0.06	57.14 %
Household 8	0.35	0.16	0.33	0.12	5.71 %	0.28	0.10	19.99 %	0.24	0.09	31.42 %	0.20	0.08	42.85 %
Household 9	0.30	0.12	0.26	0.09	13.33 %	0.24	0.08	20.00 %	0.21	0.07	30.00 %	0.18	0.07	40.00 %
Average	0.35	0.15	0.27	0.10	21.41 %	0.23	0.09	32.18 %	0.20	0.07	42.68 %	0.17	0.06	50.16 %

deviation (STD) to check the variability of the errors during the evaluation period. In the case of active and passive approaches, an additional column represents the improvement (Imp) with respect to the prediction error reduction compared to the baseline model. For households without drift detection, see Fig. 5, the baseline model is used without any adaptation.

Setting the significance level to a higher value increases the sensitivity to drift. This triggers more adaptation events, leading to an improvement in prediction quality (that is, a reduction in MAPE and RMSE). From the Tables 4 and 5, we can see that the passive approach consistently outperforms all other approaches in all households. On average, the passive approach improves the MAPE metric of all households produced by the baseline approach by 40.90 %, and the RMSE metric by 50.16 %.

Specifically, the improvement in MAPE reaches 64.03% for Household 9, while it reaches 58.33% for Household 2 on RMSE. However, for active approaches, the percentage of improvement increases with higher significance levels. The average percentage of improvement of MAPE is 8.62 % for the active approach with a significance level of $\tau = 0.07$, reaching 24.98 % for $\tau = 0.15$. We observe a similar pattern of improvement in the RMSE metric, but with a larger effect size. For $\tau = 0.07$ the improvement is 21.41 % and reaches 42.68 % for $\tau = 0.15$.

To evaluate performance on a more granular level, we plotted the daily performance metrics for two examples of each type of household. Fig. 6a and Fig. 6c present the daily MAPE and RMSE for Household 1, respectively. While Fig. 6b and Fig. 6d present the performance metrics for Household 7. As we can see, for both households, the baseline model has the highest error rates compared to when using the drift-adaptive approaches for each day of the test data. Moreover, the error curves for DA-LSTM approaches are stacked over most days in both figures. However, in a few cases, the active approach performs better than the passive approach due to the non-determinism property of the output of neural networks [107].

DA-LSTM for Load Forecasting

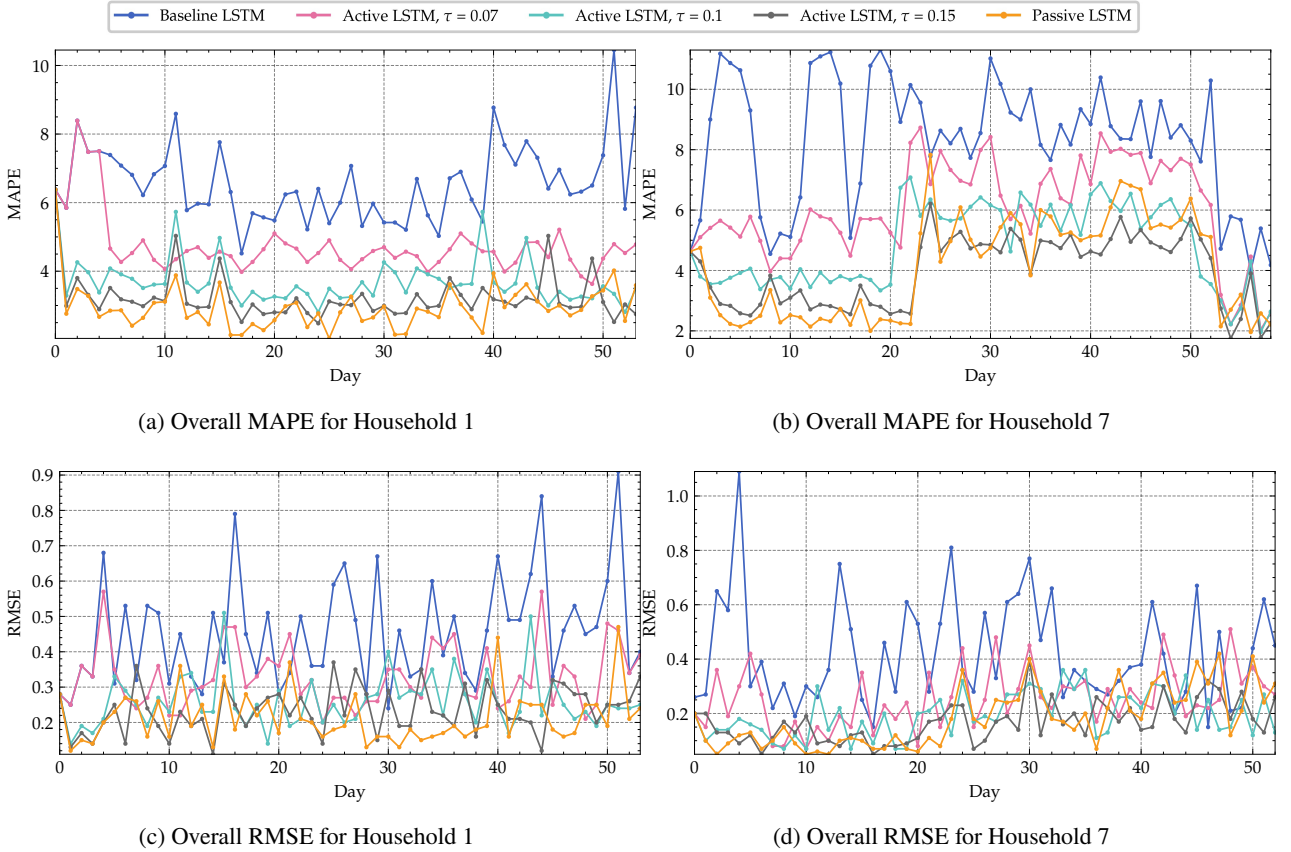


Figure 6: Performance evaluation for LSTM-based methods

5.3.2. Comparison Against Additional Baseline Methods from the Literature

To further verify the effectiveness of our proposed method, we performed additional evaluations against several commonly used baseline methods in the literature. Fig. 7a and 7b show the performance of the baseline methods and DA-LSTM on the MAPE and RMSE metrics. Regarding the non-LSTM-based baseline methods, the Bagging Regression method performs better than the RNN and ARIMA methods. Specifically, the performance of the Bagging Regression model is the most similar to the LSTM baseline model. Overall, the results show that the proposed DA-LSTM method outperforms all other baseline methods in all cases by a considerable margin for MAPE and RMSE for all households. DA-LSTM achieved a maximum improvement of 62.8% over RNN on MAPE and 84.51% on RMSE.

5.3.3. DA-LSTM Hyperparameter Optimization Results

As described in Section 3.3.1, we performed the HPO for all of the LSTM models to find the optimal parameters. Tables 6 to 9 illustrate the outcomes of hyperparameter tuning using validation data. Specifically, to provide a glimpse into the range of values that may be effective for this approach, examples of the selected hyperparameter values are reported in Tables 6 and 8 for Household 1, and Tables 7 and 9 for Household 7, with significance levels $\tau = 0.07$ and $\tau = 0.10$, respectively. In contrast to the results reported in Tables 4 and 5, which present the evaluation results for Household 1 and 7 respectively and are aggregated for the entire test dataset of each household. The tables represent the best combination of hyperparameters that resulted in the optimal performance in terms of loss value (MAPE). An interesting observation is that some hyperparameters, such as LR and DR, appear to have similar values across different detection numbers. For example, in Table 7, detection numbers 1, 6, 10, and 16 all have the same LR and DR values of 0.001 and 0.4, respectively. Similarly, in Table 9, detection numbers 1, 9, 17, and 23 have the same LR and DR values. On the contrary, the parameter N_U exhibits greater variability in different detection numbers than the other hyperparameters, suggesting that it is more sensitive to data changes.

DA-LSTM for Load Forecasting

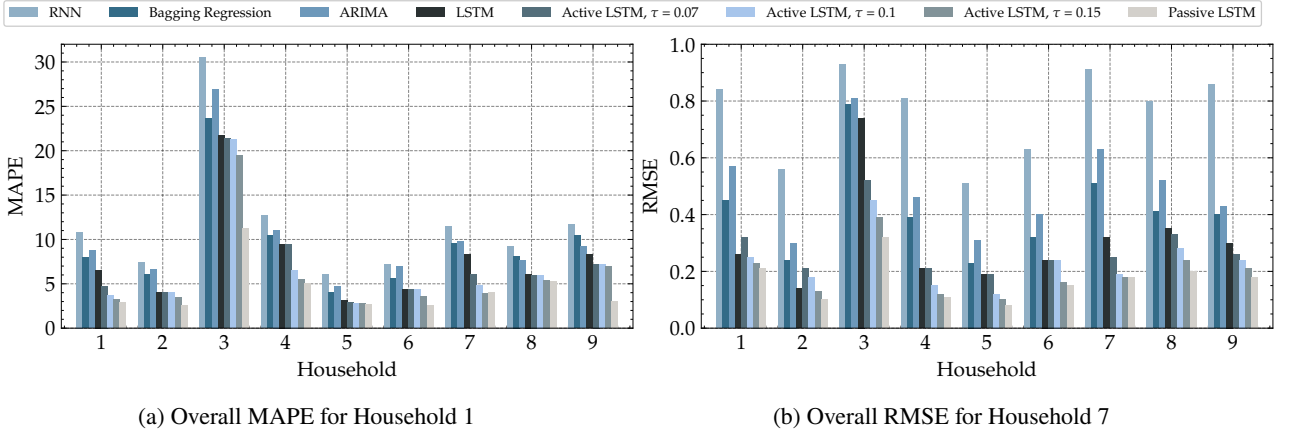


Figure 7: Performance evaluation for baseline and DA-LSTM methods

Table 6

DA-LSTM Hyperparameter values for Household 1, $\tau = 0.07$

Detection Number	LR	DR	N_U	Loss
1	0.001	0.4	192	3.13
2	0.0001	0	160	3.14
3	0.001	0.3	160	3.12
4	0.001	0.3	192	3.10
5	0.0001	0	128	3.10
6	0.0001	0	256	3.08
7	0.001	0.2	224	3.07
8	0.001	0.1	256	3.05
9	0.0001	0	192	3.05
10	0.001	0.4	192	3.00

Table 7

DA-LSTM Hyperparameter values for Household 7, $\tau = 0.07$

Detection Number	LR	DR	N_U	Loss
1	0.001	0.4	224	2.74
2	0.001	0	288	2.76
3	0.0001	0	224	2.75
4	0.001	0.2	192	2.75
5	0.0001	0	224	2.75
6	0.001	0.4	320	2.75
7	0.0001	0	320	2.75
8	0.001	0.3	224	2.77
9	0.0001	0	480	2.79
10	0.001	0.4	224	2.79
11	0.0001	0.1	384	2.81
12	0.0001	0.2	320	2.84
13	0.001	0	480	2.83
14	0.001	0.3	224	2.82
15	0.0001	0.1	416	2.83
16	0.001	0.4	320	2.83
17	0.001	0	320	2.85
18	0.0001	0	224	2.88
19	0.01	0	256	2.88
20	0.001	0.2	256	2.87

5.3.4. Learning Curves for LSTM-Based Methods

To corroborate the performance during the training process, we analyze the learning curves to inspect whether the LSTM-based models are overfitting or underfitting. Figs. 8a and 8b illustrate the training and validation curves for Household 1 and Household 7, respectively. The curves show that the model can capture the patterns in the training data without overemphasizing noise, while still being able to generalize to new data as seen in the validation set and

Table 8
DA-LSTM Hyperparameter values for Household 1, $\tau = 0.10$

Detection Number	LR	DR	N_U	Loss
1	0.01	0	96	3.17
2	0.001	0.4	256	3.24
3	0.001	0	288	3.14
4	0.001	0.3	288	3.10
5	0.0001	0.1	224	3.40
6	0.0001	0.2	224	3.79
7	0.0001	0.1	224	3.24
8	0.001	0.1	288	3.69
9	0.001	0.2	256	3.08
10	0.001	0	288	3.12
11	0.0001	0.1	256	3.18
12	0.0001	0	224	3.68
13	0.001	0.4	352	2.99
14	0.001	0.1	192	3.00
15	0.0001	0	288	2.98

Table 9
DA-LSTM Hyperparameter values for Household 7, $\tau = 0.10$

Detection Number	LR	DR	N_U	Loss
1	0.001	0.4	224	4.36
2	0.001	0	288	2.74
3	0.0001	0	224	2.74
4	0.0001	0	288	2.75
5	0.001	0.2	192	3.47
6	0.001	0	224	2.77
7	0.0001	0	224	2.74
8	0.001	0.2	480	2.76
9	0.001	0.4	320	2.76
10	0.001	0	448	2.77
11	0.0001	0	320	2.78
12	0.001	0	224	2.79
13	0.001	0	480	3.16
14	0.001	0	448	2.82
15	0.001	0.3	224	4.29
16	0.0001	0	480	2.83
17	0.001	0.4	224	2.83
18	0.0001	0.1	384	2.84
19	0.0001	0.2	320	2.83
20	0.001	0	480	2.83
21	0.001	0.3	224	2.84
22	0.0001	0.1	416	2.85
23	0.001	0.4	320	2.87
24	0.001	0	256	2.89
25	0.0001	0	352	2.88
26	0.0001	0	288	2.88
27	0.0001	0	352	2.89
28	0.0001	0	128	2.88
29	0.001	0	320	2.89
30	0.0001	0	224	2.89
31	0.01	0	256	2.87
32	0.001	0.2	256	2.87

there is no specific sign of over- or under-fitting.

5.4. Computational Cost

Adjusting the models to adapt to changes is associated with additional computational costs. Figs. 9 and 10 present the CPU and GPU usage for each of the active and passive approaches of Household 7; the household with the highest number of detected drifts. As can be seen, when the adaptation signal is activated due to a change in behavior, we have a similar resource utilization pattern in both approaches. For CPU, it fluctuates between 7% and 10% per thread, while for GPU, the utilization of resources is between 45% and 60%. The conventional LSTM model, as described in Section 3.2, only computes sequentially. But both TensorFlow and PyTorch introduced a cuDNNLSTM wrapper⁴ for

⁴cuDNNLSTM: https://www.tensorflow.org/api_docs/python/tf/compat/v1/keras/layers/CuDNNLSTM

DA-LSTM for Load Forecasting

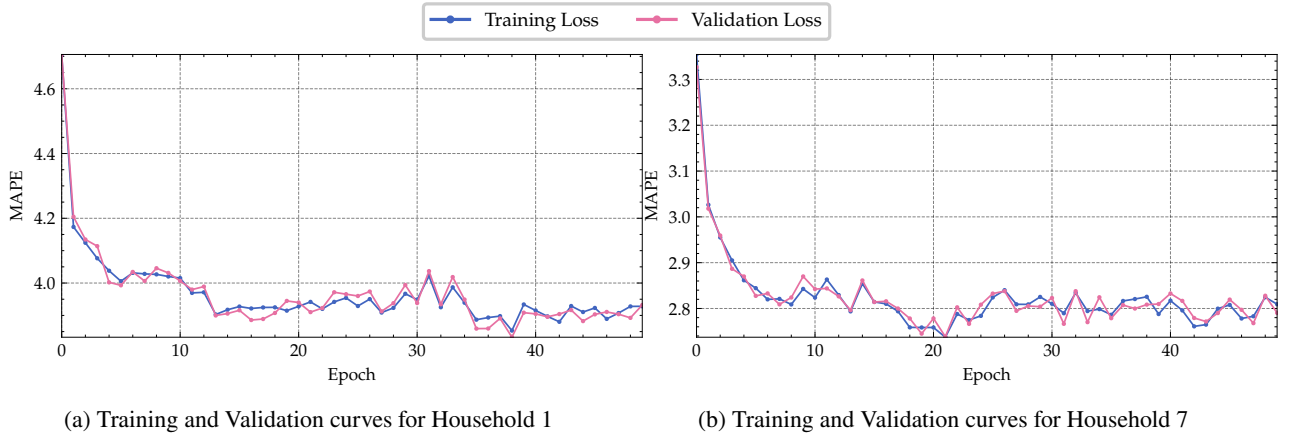


Figure 8: Training and validation curves

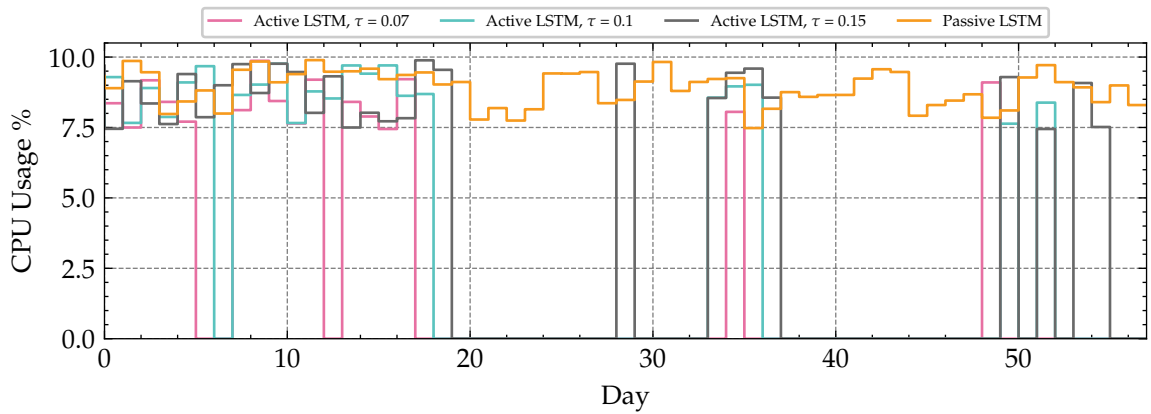


Figure 9: Daily CPU usage percentage of forecasting model for Household 7

the normal LSTM implementation, which enables its partly parallelization [108, 109]

In Table 10, the total AWS costs in Euros for the entire evaluation period of each household are presented. The cost is calculated based on the number of minutes needed for the adaptation with the on-demand pricing of the instance. The table shows that the passive approach is at least twice as costly as the active approach with the selected significance levels. On the daily level, Fig. 11 shows the computational cost for Household 7 to adapt the model on the AWS instance. As can be seen, the passive approach shows a constant cost throughout the whole observed evaluation period. This is because the training time and hyperparameter tuning for each daily period require the same timeframe. However, the active approaches impose a variable cost. For example, when $\tau = 0.07$, a significant change in computational cost can be observed on day 37 with a cost of 0.744 for the training in ML adaptation. This increase in cost occurs when the time between changes is prolonged, leading to a more extensive training dataset for the adaptation of LSTM and, consequently, to higher costs. The total cost of running the system for 58 consecutive days for the passive approach is 15.93 Euros, which corresponds to 0.27 per day. In comparison, the cost for the same period when using the active approaches are: 5.96, 6.67, and 8.44 with an increasing τ , respectively. It is visible that even with a single household over the time span of only 58 days, the proposed approach can save about 53% of the computational cost with $\tau = 0.15$. Scaling the number of households in a typical case of only one low voltage feeder of tens of households, e.g., 70 households, the savings in practice are even much higher in the case of several low voltage feeders on a residential region of some hundreds of residencies. Thus, this method would result in high savings in terms of costs.

DA-LSTM for Load Forecasting

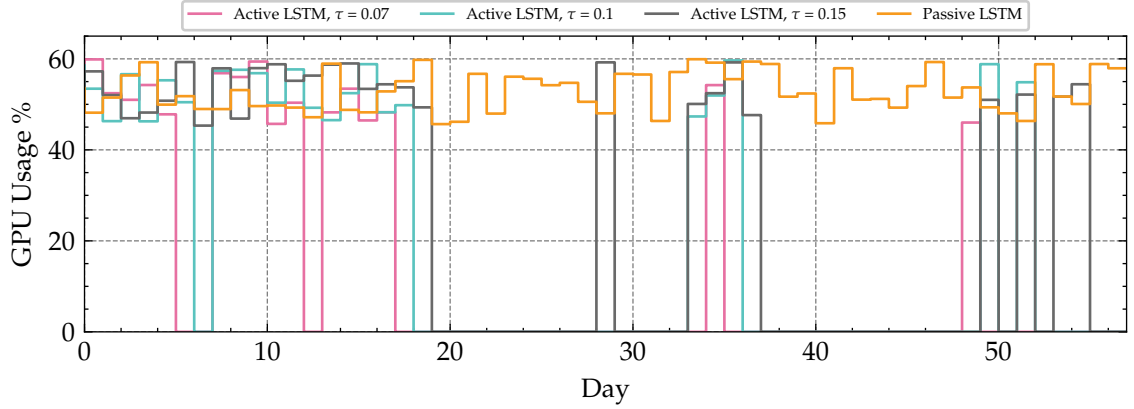


Figure 10: Daily GPU usage percentage of forecasting model for Household 7

Table 10

Total computational cost per household in EUR

Household	$\tau = 0.07$	$\tau = 0.10$	$\tau = 0.15$	Passive
Household 1	7.53	8.86	9.88	24.17
Household 2	7.44	8.11	11.02	31.31
Household 3	4.56	5.50	6.50	26.37
Household 4	0.00	4.10	4.91	22.80
Household 5	0.00	7.66	9.89	18.95
Household 6	0.00	0.00	2.52	20.60
Household 7	5.96	6.68	8.45	15.93
Household 8	9.42	10.56	12.56	31.04
Household 9	7.27	9.25	10.47	20.60

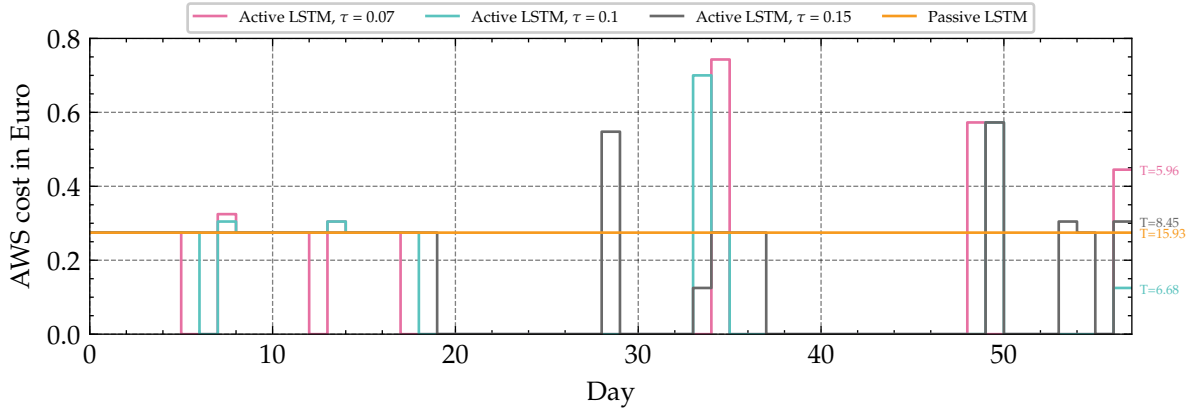


Figure 11: Daily AWS cost of forecasting model for Household 7, T is the total cost of the entire period

5.5. Performance-Cost Trade-off

In the previous section, it was evident that there is a trade-off between predictive performance and the associated computational cost of each approach. In most cases, the passive approach is the most powerful approach in terms of prediction accuracy. However, at the same time, it is the most expensive approach in terms of computational costs. Similarly, the active approach showed behaviors identical to those of the passive approach. Effective approaches are associated with additional workload costs due to the number of adaptation events. We have calculated a metric that combines predictive performance and computational costs to further analyze the trade-off.

The simplest measure that combines both performance and costs is the ratio between the two metrics [110]. The

Table 11

Trade-off metric between performance improvement and cost

Household	$\tau = 0.07$	$\tau = 0.10$	$\tau = 0.15$	Passive
Household 1	3.68	4.92	5.15*	2.28
Household 2	0.07	0.09	1.23*	1.2
Household 3	0.28	0.39	1.58	1.83*
Household 4	0.00	7.57	8.44*	2.03
Household 5	0.00	1.39*	1.11	0.73
Household 6	0.00	0.00	6.87*	1.92
Household 7	4.62	6.34*	6.23	3.19
Household 8	0.17	0.16	0.89*	0.41
Household 9	1.88	1.53	1.58	3.11*

trade-off score (TS) can be simply calculated as follows:

$$TS = \frac{\text{Performance}}{\text{Cost}}, \quad (15)$$

where Performance is the metric that is used to evaluate the predictive performance of the approach, we chose the MAPE metric as it yielded similar results to RMSE, and cost is the total cost of the associated AWS instance for the evaluation period. The most efficient approach is one that maximizes performance per unit cost ratio (TS). Table 11 presents the results in the household of computing the trade-off metric for each approach. The metric is calculated based on the improvement of the error rate (shown in Table 4) and the total cost of the AWS instance (shown in Table 10).

We can see that there is no single approach that fits all household data. However, the results show that the active strategy with a significance level of $\tau = 0.15$ is the most efficient approach in terms of the TS metric for five out of nine households. Meanwhile, despite its low error rate, the passive strategy is the most effective approach for two households only. This means that the additional costs do not move proportionally with the performance improvement rates. Furthermore, the active strategy with a significance level of $\tau = 0.1$ has been the most effective approach for two households in total.

5.6. Discussion

In this section, we presented a detailed experimental evaluation of the performance of DA-LSTM using a real-life dataset. Our DA-LSTM approach introduces a novel adaptive mechanism that dynamically adjusts the LSTM model to changing data patterns, allowing for accurate and robust predictions in the presence of concept drift. We employed an active-based drift detection approach, which leverages statistical significance testing, to detect drift events and trigger model adaptations accordingly. This active approach is a key contribution of our work, as it enables the LSTM model to dynamically adapt to changes and maintain high prediction performance over time. Additionally, compared to other drift adaptive methods in interval load forecasting such as [103, 40, 43], which require setting a threshold for drift magnitude, the dynamic drift detection methodology implemented in the proposed method is a flexible tool for detecting changes in consumption patterns without pre-defining a threshold. As it can be challenging to determine an appropriate threshold for drift detection in real-life settings. This feature adds to the practicality and usefulness of the proposed method in real-world applications. Moreover, the incremental learning technique employed in our DA-LSTM approach is advantageous as it builds on the previously learned knowledge and avoids the shortcomings of complete forgetting, as required in some studies that only rely on the most recent observations as a prerequisite [42, 111], and hence cannot leverage old patterns that may reappear.

The results of our experiments clearly demonstrate that our DA-LSTM model significantly outperforms commonly used baseline methods in terms of prediction accuracy, while also achieving a reasonable trade-off between performance and computational cost. In terms of prediction performance, the passive LSTM approach showed superior results compared to other methods in terms of MAPE and RMSE metrics, with notable average improvements across all households. The active approach also exhibited higher prediction performance, with average improvements for a significance level of $\tau = 0.07$ and even higher improvements for $\tau = 0.15$. Furthermore, our DA-LSTM method surpassed other commonly used baseline methods from the literature, such as RNN, ARIMA, and Bagging Regression, by a significant margin in terms of MAPE and RMSE for all households.

By comparing the performance-cost trade-off results of the different methods, we could gain deeper insights into which method might be best suited for different use cases. Specifically, we found that the active approach yielded a

better overall trade-off performance than the passive approach. This suggests that the active approach could be more suitable in scenarios where computational cost is a determinative factor. Another important advantage of the active LSTM approach is its interpretability. Active detection provides additional information about change points in the time-series data, allowing for a better understanding of the underlying dynamics driving the consumption patterns. This interpretability can be particularly useful for power utility companies in real-world applications, where it is important to have insights into why and when changes in consumption occur. In contrast, passive adaptation provides more accurate predictive capabilities but at the cost of higher computational burden and limited interpretability due to the lack of information on changes in the data.

5.7. Limitations and Outlook

To assess the proposed framework, we evaluated the framework for the load forecasting use case with LSTM models. However, the framework is not limited to these settings, and the drift-adaptation methodology is model-agnostic and can be integrated with any ML-based predictor. Furthermore, the framework can be applied to other data types. In the multivariate case, the divergence metric will be calculated based on a multivariate probability density function. Additionally, the predictive model should support multiple inputs in the input layer that we would investigate in future work. For drift magnitude sensitivity, the TS metric could be a useful indicator that helps in selecting the most appropriate approach for the corresponding problem. However, some limitations may also affect the adoption of the appropriate approach, such as a threshold for minimum desired performance or budget allocations for costs.

6. Conclusion

DL techniques have been exploited in the problem of interval load forecasting of residential households. Most existing solutions use offline learning, where the solution is built using historical data and deployed once it achieves good results with training data. This solution does not guarantee good performance after deployment since changes could occur and the solution would be obsolete. This paper proposes a drift-adaptive framework for LSTM networks (DA-LSTM) that can dynamically detect and adapt to changes. The main characteristic of the proposed framework is that it does not require fixing a drift threshold, since it evolves with time dynamically using the drift magnitude distribution. We integrate several detection strategies and apply them to real-world datasets. The evaluation is carried out in terms of prediction performance using MAPE and RMSE metrics, and the associated computational costs of using CPU and GPU resources. Additionally, the costs of using a cloud-based service (AWS) are calculated to quantify the deployment costs. The evaluation results demonstrate the efficiency of our solution compared to conventional LSTM and other popular baseline methods in terms of prediction performance. We also present an analysis of the trade-off between the performance and costs of each approach that would provide suggestions for adopting the appropriate approach in real-life problems.

Acknowledgement

This work has been partially funded by the Knowledge Foundation of Sweden (KKS) through the Synergy Project AIDA - A Holistic AI-driven Networking and Processing Framework for Industrial IoT (Rek:20200067). Additional funding has been provided by the Swedish Energy Agency through the AI4-ENERGI project (grant number 50246-1) and the project Solar Electricity Research Centre, Sweden (SOLVE), grant number 52693-1.

References

- [1] Dasheng Lee and Chin-Chi Cheng. Energy savings by energy management systems: A review. *Renewable and Sustainable Energy Reviews*, 56:760–777, 2016.
- [2] Barb Martin and Tom Ries. Managing energy helps optimize a distribution system. *Opflow*, 40(12):8–9, 2014.
- [3] László Czétányi, Viktória Vámos, Miklós Horváth, Zsuzsa Szalay, Adrián Mota-Babiloni, Zsófia Deme-Bélafi, and Tamás Csoknyai. Development of electricity consumption profiles of residential buildings based on smart meter data clustering. *Energy and Buildings*, 252:111376, 2021.
- [4] Baran Yildiz, Jose I Bilbao, Jonathon Dore, and Alistair B Sproul. Recent advances in the analysis of residential electricity consumption and applications of smart meter data. *Applied Energy*, 208:402–427, 2017.
- [5] Ismail Shah, Hasnain Iftikhar, and Sajid Ali. Modeling and forecasting medium-term electricity consumption using component estimation technique. *Forecasting*, 2(2):163–179, 2020.
- [6] Elias Kyriakides and Marios Polycarpou. Short term electric load forecasting: A tutorial. *Trends in Neural Computation*, pages 391–418, 2007.

- [7] John V Ringwood, D Bofelli, and Fiona T Murray. Forecasting electricity demand on short, medium and long time scales using neural networks. *Journal of Intelligent and Robotic Systems*, 31(1):129–147, 2001.
- [8] Patrick E McSharry, Sonja Bouwman, and Gabriël Bloemhof. Probabilistic forecasts of the magnitude and timing of peak electricity demand. *IEEE Transactions on Power Systems*, 20(2):1166–1172, 2005.
- [9] Arjun Baliyan, Kumar Gaurav, and Sudhansu Kumar Mishra. A review of short term load forecasting using artificial neural network models. *Procedia Computer Science*, 48:121–125, 2015.
- [10] Juan J Cárdenas, Luis Romeral, Antonio Garcia, and Fabio Andrade. Load forecasting framework of electricity consumptions for an intelligent energy management system in the user-side. *Expert Systems with Applications*, 39(5):5557–5565, 2012.
- [11] Jie Lu, Anjin Liu, Fan Dong, Feng Gu, Joao Gama, and Guangquan Zhang. Learning under concept drift: A review. *IEEE Transactions on Knowledge and Data Engineering*, 31(12):2346–2363, 2018.
- [12] Huaizhi Wang, Zhenxing Lei, Xian Zhang, Bin Zhou, and Jianchun Peng. A review of deep learning for renewable energy forecasting. *Energy Conversion and Management*, 198:111799, 2019.
- [13] Matteo Muratori and Giorgio Rizzoni. Residential demand response: Dynamic energy management and time-varying electricity pricing. *IEEE Transactions on Power systems*, 31(2):1108–1117, 2015.
- [14] Mohamed H Albadi and Ehab F El-Saadany. Demand response in electricity markets: An overview. In *2007 IEEE power engineering society general meeting*, pages 1–5. IEEE, 2007.
- [15] Shahida Khatoon, Arunesh Kr Singh, et al. Effects of various factors on electric load forecasting: An overview. In *2014 6th IEEE Power India International Conference (PIICON)*, pages 1–5. IEEE, 2014.
- [16] Firas Bayram, Bestoun S Ahmed, and Andreas Kassler. From concept drift to model degradation: An overview on performance-aware drift detectors. *Knowledge-Based Systems*, page 108632, 2022.
- [17] Yunxuan Dong, Xuejiao Ma, and Tonglin Fu. Electrical load forecasting: A deep learning approach based on k-nearest neighbors. *Applied Soft Computing*, 99:106900, 2021.
- [18] Sima Siami-Namini, Neda Tavakoli, and Akbar Siami Namin. A comparison of arima and lstm in forecasting time series. In *2018 17th IEEE international conference on machine learning and applications (ICMLA)*, pages 1394–1401. IEEE, 2018.
- [19] Tingting Hou, Rengcun Fang, Jinrui Tang, Ganheng Ge, Dongjun Yang, Jianchao Liu, and Wei Zhang. A novel short-term residential electric load forecasting method based on adaptive load aggregation and deep learning algorithms. *Energies*, 14(22):7820, 2021.
- [20] Geoffrey I Webb, Roy Hyde, Hong Cao, Hai Long Nguyen, and Francois Petitjean. Characterizing concept drift. *Data Mining and Knowledge Discovery*, 30(4):964–994, 2016.
- [21] Scott Wares, John Isaacs, and Eyad Elyan. Data stream mining: methods and challenges for handling concept drift. *SN Applied Sciences*, 1(11):1–19, 2019.
- [22] Anjin Liu, Jie Lu, Yiliao Song, Junyu Xuan, and Guangquan Zhang. Concept drift detection delay index. *IEEE Transactions on Knowledge and Data Engineering*, 2022.
- [23] Corentin Kuster, Yacine Rezugui, and Monjur Mourshed. Electrical load forecasting models: A critical systematic review. *Sustainable Cities and Society*, 35:257–270, 2017.
- [24] Bishnu Nepal, Motoi Yamaha, Aya Yokoe, and Toshiya Yamaji. Electricity load forecasting using clustering and arima model for energy management in buildings. *Japan Architectural Review*, 3(1):62–76, 2020.
- [25] Luis Hernández, Carlos Baladrón, Javier M Aguiar, Belén Carro, Antonio Sánchez-Esguevillas, and Jaime Lloret. Artificial neural networks for short-term load forecasting in microgrids environment. *Energy*, 75:252–264, 2014.
- [26] Ye Hong, Yingjie Zhou, Qibin Li, Wenzheng Xu, and Xiujian Zheng. A deep learning method for short-term residential load forecasting in smart grid. *IEEE Access*, 8:55785–55797, 2020.
- [27] Ljubisa Sehovac and Katarina Grolinger. Deep learning for load forecasting: Sequence to sequence recurrent neural networks with attention. *IEEE Access*, 8:36411–36426, 2020.
- [28] Ashish Vaswani, Noam Shazeer, Niki Parmar, Jakob Uszkoreit, Llion Jones, Aidan N Gomez, Łukasz Kaiser, and Illia Polosukhin. Attention is all you need. *Advances in neural information processing systems*, 30, 2017.
- [29] Venkataramana Veeramsetty, Dongari Rakesh Chandra, Francesco Grimaccia, and Marco Mussetta. Short term electric power load forecasting using principal component analysis and recurrent neural networks. *Forecasting*, 4(1):149–164, 2022.
- [30] Haixiang Zang, Ruiqi Xu, Lilin Cheng, Tao Ding, Ling Liu, Zhinong Wei, and Guoqiang Sun. Residential load forecasting based on lstm fusing self-attention mechanism with pooling. *Energy*, 229:120682, 2021.
- [31] Hosein Eskandari, Maryam Imani, and Mohsen Parsa Moghaddam. Convolutional and recurrent neural network based model for short-term load forecasting. *Electric Power Systems Research*, 195:107173, 2021.
- [32] Shafiqul Hasan Rafi, Shohana Rahman Deeba, Eklas Hossain, et al. A short-term load forecasting method using integrated cnn and lstm network. *IEEE Access*, 9:32436–32448, 2021.
- [33] Hui Hwang Goh, Biliang He, Hui Liu, Dongdong Zhang, Wei Dai, Tonni Agustiono Kurniawan, and Kai Chen Goh. Multi-convolution feature extraction and recurrent neural network dependent model for short-term load forecasting. *IEEE Access*, 9:118528–118540, 2021.
- [34] Nivethitha Somu, Gauthama Raman MR, and Krithi Ramamritham. A deep learning framework for building energy consumption forecast. *Renewable and Sustainable Energy Reviews*, 137:110591, 2021.
- [35] Xianlun Tang, Hongxu Chen, Wenhao Xiang, Jingming Yang, and Mi Zou. Short-term load forecasting using channel and temporal attention based temporal convolutional network. *Electric Power Systems Research*, 205:107761, 2022.
- [36] Jiancai Song, Guixiang Xue, Xuhua Pan, Yunpeng Ma, and Han Li. Hourly heat load prediction model based on temporal convolutional neural network. *IEEE Access*, 8:16726–16741, 2020.
- [37] Aoqi Xu, Man-Wen Tian, Behnam Firouzi, Khalid A Alattas, Ardashir Mohammadzadeh, and Ebrahim Ghaderpour. A new deep learning restricted boltzmann machine for energy consumption forecasting. *Sustainability*, 14(16):10081, 2022.
- [38] Abdul Azeem, Idris Ismail, Syed Muslim Jameel, Fakhizan Romlie, Kamaluddeen Usman Danyaro, and Saurabh Shukla. Deterioration of

- electrical load forecasting models in a smart grid environment. *Sensors*, 22(12):4363, 2022.
- [39] Mohammad Navid Fekri, Harsh Patel, Katarina Grolinger, and Vinay Sharma. Deep learning for load forecasting with smart meter data: Online adaptive recurrent neural network. *Applied Energy*, 282:116177, 2021.
- [40] Rashpinder Kaur Jagait, Mohammad Navid Fekri, Katarina Grolinger, and Syed Mir. Load forecasting under concept drift: Online ensemble learning with recurrent neural network and arima. *IEEE Access*, 9:98992–99008, 2021.
- [41] Gabriela Grmanová, Peter Laurinec, Viera Rozinajová, Anna Bou Ezzeddine, Mária Lucká, Peter Lacko, Petra Vrablecová, and Pavol Návrat. Incremental ensemble learning for electricity load forecasting. *Acta Polytechnica Hungarica*, 13(2):97–117, 2016.
- [42] Giuseppe Fenza, Mariacristina Gallo, and Vincenzo Loia. Drift-aware methodology for anomaly detection in smart grid. *IEEE Access*, 7:9645–9657, 2019.
- [43] Yuanfan Ji, Guangchao Geng, and Quanyuan Jiang. Enhancing model adaptability using concept drift detection for short-term load forecast. In *2021 IEEE/IAS Industrial and Commercial Power System Asia (I&CPS Asia)*, pages 464–469. IEEE, 2021.
- [44] Albert Bifet and Ricard Gavaldà. Learning from time-changing data with adaptive windowing. In *Proceedings of the 2007 SIAM international conference on data mining*, pages 443–448. SIAM, 2007.
- [45] David Obst, Joseph de Vilmares, and Yannig Goüde. Adaptive methods for short-term electricity load forecasting during covid-19 lockdown in france. *IEEE Transactions on Power Systems*, 36(5):4754–4763, 2021.
- [46] Alexey Tsymbal. The problem of concept drift: definitions and related work. *Computer Science Department, Trinity College Dublin*, 106(2):58, 2004.
- [47] Gregory Ditzler, Manuel Roveri, Cesare Alippi, and Robi Polikar. Learning in nonstationary environments: A survey. *IEEE Computational Intelligence Magazine*, 10(4):12–25, 2015.
- [48] Yiliao Song, Jie Lu, Anjin Liu, Haiyan Lu, and Guangquan Zhang. A segment-based drift adaptation method for data streams. *IEEE transactions on neural networks and learning systems*, 2021.
- [49] Imen Khamassi, Moamar Sayed-Mouchaweh, Moez Hammami, and Khaled Ghédira. Discussion and review on evolving data streams and concept drift adapting. *Evolving systems*, 9(1):1–23, 2018.
- [50] Fan Dong, Jie Lu, Yiliao Song, Feng Liu, and Guangquan Zhang. A drift region-based data sample filtering method. *IEEE Transactions on Cybernetics*, 2021.
- [51] Song Liu, Makoto Yamada, Nigel Collier, and Masashi Sugiyama. Change-point detection in time-series data by relative density-ratio estimation. *Neural Networks*, 43:72–83, 2013.
- [52] Bartosz Krawczyk, Leandro L Minku, João Gama, Jerzy Stefanowski, and Michał Woźniak. Ensemble learning for data stream analysis: A survey. *Information Fusion*, 37:132–156, 2017.
- [53] Johannes Haug and Gjergji Kasneci. Learning parameter distributions to detect concept drift in data streams. In *2020 25th International Conference on Pattern Recognition (ICPR)*, pages 9452–9459. IEEE, 2021.
- [54] Yoshinobu Kawahara and Masashi Sugiyama. Sequential change-point detection based on direct density-ratio estimation. *Stat. Anal. Data Min.*, 5(2):114–127, apr 2012.
- [55] Yang Zhao, Chaobo Zhang, Yiwen Zhang, Zihao Wang, and Junyang Li. A review of data mining technologies in building energy systems: Load prediction, pattern identification, fault detection and diagnosis. *Energy and Built Environment*, 1(2):149–164, 2020.
- [56] Shengzeng Li, Yiwen Zhong, and Jiayang Lin. Aws-daie: Incremental ensemble short-term electricity load forecasting based on sample domain adaptation. *Sustainability*, 14(21):14205, 2022.
- [57] Weicong Kong, Zhao Yang Dong, David J Hill, Fengji Luo, and Yan Xu. Short-term residential load forecasting based on resident behaviour learning. *IEEE Transactions on Power Systems*, 33(1):1087–1088, 2017.
- [58] Lillian Lee. Measures of distributional similarity. *arXiv preprint cs/0001012*, 2000.
- [59] João Gama, Indrė Žliobaitė, Albert Bifet, Mykola Pechenizkiy, and Abdelhamid Bouchachia. A survey on concept drift adaptation. *ACM computing surveys (CSUR)*, 46(4):1–37, 2014.
- [60] Dominik Maria Endres and Johannes E Schindelin. A new metric for probability distributions. *IEEE Transactions on Information theory*, 49(7):1858–1860, 2003.
- [61] Jianhua Lin. Divergence measures based on the shannon entropy. *IEEE Transactions on Information theory*, 37(1):145–151, 1991.
- [62] Timothy P Burke, Brian C Kiedrowski, and William R Martin. Kernel density estimation of reaction rates in neutron transport simulations of nuclear reactors. *Nuclear Science and Engineering*, 188(2):109–139, 2017.
- [63] Kaushik Banerjee and William R Martin. Kernel density estimation method for monte carlo global flux tallies. *Nuclear science and engineering*, 170(3):234–250, 2012.
- [64] Yen-Chi Chen. A tutorial on kernel density estimation and recent advances. *Biostatistics & Epidemiology*, 1(1):161–187, 2017.
- [65] Taoufik Bouezmarni and Olivier Scaillet. Consistency of asymmetric kernel density estimators and smoothed histograms with application to income data. *Econometric Theory*, 21(2):390–412, 2005.
- [66] Bernard W Silverman. *Density estimation for statistics and data analysis*. Routledge, 2018.
- [67] Larry Wasserman. *All of nonparametric statistics*. Springer Science & Business Media, 2006.
- [68] David W Scott. *Multivariate density estimation: theory, practice, and visualization*. John Wiley & Sons, 2015.
- [69] Shean-Tsong Chiu. A comparative review of bandwidth selection for kernel density estimation. *Statistica Sinica*, pages 129–145, 1996.
- [70] Chengjin Ye, Yi Ding, Peng Wang, and Zhenzhi Lin. A data-driven bottom-up approach for spatial and temporal electric load forecasting. *IEEE Transactions on Power Systems*, 34(3):1966–1979, 2019.
- [71] Josh Patterson and Adam Gibson. *Deep learning: A practitioner's approach*. " O'Reilly Media, Inc.", 2017.
- [72] Yong Yu, Xiaosheng Si, Changhua Hu, and Jianxun Zhang. A review of recurrent neural networks: Lstm cells and network architectures. *Neural computation*, 31(7):1235–1270, 2019.
- [73] Kyunghyun Cho, Bart Van Merriënboer, Caglar Gulcehre, Dzmitry Bahdanau, Fethi Bougares, Holger Schwenk, and Yoshua Bengio. Learning phrase representations using rnn encoder-decoder for statistical machine translation. *arXiv preprint arXiv:1406.1078*, 2014.

- [74] Apeksha Shewalkar. Performance evaluation of deep neural networks applied to speech recognition: Rnn, lstm and gru. *Journal of Artificial Intelligence and Soft Computing Research*, 9(4):235–245, 2019.
- [75] Sepp Hochreiter and Jürgen Schmidhuber. Long short-term memory. *Neural computation*, 9(8):1735–1780, 1997.
- [76] Martin Sundermeyer, Ralf Schlüter, and Hermann Ney. Lstm neural networks for language modeling. In *Thirteenth annual conference of the international speech communication association*, 2012.
- [77] Felix A Gers, Jürgen Schmidhuber, and Fred Cummins. Learning to forget: Continual prediction with lstm. *Neural computation*, 12(10):2451–2471, 2000.
- [78] Wenyu Zang, Peng Zhang, Chuan Zhou, and Li Guo. Comparative study between incremental and ensemble learning on data streams: Case study. *Journal of Big Data*, 1(1):1–16, 2014.
- [79] RR Ade and PR Deshmukh. Methods for incremental learning: a survey. *International Journal of Data Mining & Knowledge Management Process*, 3(4):119, 2013.
- [80] Zhi-Hua Zhou and Zhao-Qian Chen. Hybrid decision tree. *Knowledge-based systems*, 15(8):515–528, 2002.
- [81] Xin Xu, Wei Wang, and Jianhong Wang. A three-way incremental-learning algorithm for radar emitter identification. *Frontiers of Computer Science*, 10(4):673–688, 2016.
- [82] Steffen Lange and Sandra Zilles. Formal models of incremental learning and their analysis. In *Proceedings of the International Joint Conference on Neural Networks, 2003.*, volume 4, pages 2691–2696. IEEE, 2003.
- [83] Christophe Giraud-Carrier. A note on the utility of incremental learning. *Ai Communications*, 13(4):215–223, 2000.
- [84] Ching-Yi Hung, Cheng-Hao Tu, Cheng-En Wu, Chien-Hung Chen, Yi-Ming Chan, and Chu-Song Chen. Compacting, picking and growing for unforgetting continual learning. *Advances in Neural Information Processing Systems*, 32, 2019.
- [85] Youlu Xing, Xiaofeng Shi, Furao Shen, Ke Zhou, and Jinxi Zhao. A self-organizing incremental neural network based on local distribution learning. *Neural Networks*, 84:143–160, 2016.
- [86] Maisnam Niranjana Singh and Samitha Khaiyum. Enhanced data stream classification by optimized weight updated meta-learning: continuous learning-based on concept-drift. *International Journal of Web Information Systems*, 2021.
- [87] Wan He. Load forecasting via deep neural networks. *Procedia Computer Science*, 122:308–314, 2017.
- [88] Matthias Feurer and Frank Hutter. Hyperparameter optimization. In *Automated machine learning*, pages 3–33. Springer, Cham, 2019.
- [89] Gábor Melis, Chris Dyer, and Phil Blunsom. On the state of the art of evaluation in neural language models. *arXiv preprint arXiv:1707.05589*, 2017.
- [90] Douglas C Montgomery. *Design and analysis of experiments*. John Wiley & sons, 2017.
- [91] James Bergstra, Rémi Bardenet, Yoshua Bengio, and Balázs Kégl. Algorithms for hyper-parameter optimization. *Advances in neural information processing systems*, 24, 2011.
- [92] Klaus Greff, Rupesh K Srivastava, Jan Koutník, Bas R Steunebrink, and Jürgen Schmidhuber. Lstm: A search space odyssey. *IEEE transactions on neural networks and learning systems*, 28(10):2222–2232, 2016.
- [93] Álvaro C Lemos Neto, Rodrigo A Coelho, and Cristiano L de Castro. An incremental learning approach using long short-term memory neural networks. *Journal of Control, Automation and Electrical Systems*, pages 1–9, 2022.
- [94] Geoffrey I Webb, Loong Kuan Lee, Bart Goethals, and François Petitjean. Analyzing concept drift and shift from sample data. *Data Mining and Knowledge Discovery*, 32(5):1179–1199, 2018.
- [95] Rishabh K Jain, Kevin M Smith, Patricia J Culligan, and John E Taylor. Forecasting energy consumption of multi-family residential buildings using support vector regression: Investigating the impact of temporal and spatial monitoring granularity on performance accuracy. *Applied Energy*, 123:168–178, 2014.
- [96] Huan Long, Zijun Zhang, and Yan Su. Analysis of daily solar power prediction with data-driven approaches. *Applied Energy*, 126:29–37, 2014.
- [97] Yiliao Song, Jie Lu, Haiyan Lu, and Guangquan Zhang. Learning data streams with changing distributions and temporal dependency. *IEEE Transactions on Neural Networks and Learning Systems*, 2021.
- [98] Gregory Ditzler and Robi Polikar. Incremental learning of concept drift from streaming imbalanced data. *IEEE transactions on knowledge and data engineering*, 25(10):2283–2301, 2012.
- [99] Roberto Souto Maior Barros and Silas Garrido T Carvalho Santos. A large-scale comparison of concept drift detectors. *Information Sciences*, 451:348–370, 2018.
- [100] Theo A Knijnenburg, Lodewyk FA Wessels, Marcel JT Reinders, and Ilya Shmulevich. Fewer permutations, more accurate p-values. *Bioinformatics*, 25(12):i161–i168, 2009.
- [101] Ellysia Jumin, Faridah Bte Basaruddin, Yuzainee Bte Yusoff, Sarmad Dashti Latif, Ali Najah Ahmed, et al. Solar radiation prediction using boosted decision tree regression model: A case study in malaysia. *Environmental Science and Pollution Research*, 28(21):26571–26583, 2021.
- [102] Nikunj C Oza and Stuart J Russell. Online bagging and boosting. In *International Workshop on Artificial Intelligence and Statistics*, pages 229–236. PMLR, 2001.
- [103] Mohammad Navid Fekri, Harsh Patel, Katarina Grolinger, and Vinay Sharma. Deep learning for load forecasting with smart meter data: Online adaptive recurrent neural network. *Applied Energy*, 282:116177, 2021.
- [104] Isaac Kofi Nti, Moses Teimeh, Owusu Nyarko-Boateng, and Adebayo Felix Adekoya. Electricity load forecasting: a systematic review. *Journal of Electrical Systems and Information Technology*, 7(1):1–19, 2020.
- [105] Letisia Catherine George, Yanan Guo, Denis Stepanov, Vikas Kumar Reddy Peri, Roshan Lakmal Elvitigala, and Maria Spichkova. Usage visualisation for the aws services. *Procedia Computer Science*, 176:3710–3717, 2020.
- [106] Rezvan Pakdel and John Herbert. Adaptive cost efficient framework for cloud-based machine learning. In *2017 IEEE 41st Annual Computer Software and Applications Conference (COMPSAC)*, volume 2, pages 155–160. IEEE, 2017.
- [107] Brian J Taylor, Marjorie A Darrah, and Christina D Moats. Verification and validation of neural networks: a sampling of research in progress.

In *Intelligent Computing: Theory and Applications*, volume 5103, pages 8–16. SPIE, 2003.

- [108] Stefan Braun. Lstm benchmarks for deep learning frameworks. *arXiv preprint arXiv:1806.01818*, 2018.
- [109] Jeremy Appleyard, Tomas Kocisky, and Phil Blunsom. Optimizing performance of recurrent neural networks on gpus. *arXiv preprint arXiv:1604.01946*, 2016.
- [110] André Vandierendonck. A comparison of methods to combine speed and accuracy measures of performance: A rejoinder on the binning procedure. *Behavior research methods*, 49(2):653–673, 2017.
- [111] Gopal Chitalia, Manisa Pipattanasomporn, Vishal Garg, and Saifur Rahman. Robust short-term electrical load forecasting framework for commercial buildings using deep recurrent neural networks. *Applied Energy*, 278:115410, 2020.